Check for updates

Comparing diverse extraction methodologies to infer the performance of 1,8-cineole extraction from *Eucalyptus cinerea*: process optimization, kinetics, and interaction mechanisms†

Divya Baskaran, [ID] [ac] Madhumitha Sathiamoorthy,[b] Ramasamy Govindarasu [ID] *[b] and Hun-Soo Byun [ID] *[a]

Eucalyptus oil is highly valued for its anti-inflammatory, antiviral, and antibacterial qualities. Research has shown that it is a powerful combatant against cancer cells, making it an extremely interesting area of research. For the first time, the present study proposes to extract 1,8-cineole from *Eucalyptus cinerea* leaves using different extraction methodologies, namely, hydro-distillation (HD), Soxhlet (SE), ultrasonication (UE), and microwave (ME) extraction techniques. In conventional extraction, HD yielded a maximum of 72.85% 1,8-cineole using a minimum solid–solvent ratio of $1:10$ g mL^{-1} within 3 h compared to SE. The first-order kinetic equation was applied in the HD experimental dataset to understand the extraction mechanism. In modern extraction technology, ME achieved the highest yield of 1,8-cineole (95.62%) at the optimal solid–solvent ratio of 2 g mL^{-1}, extraction time of 4.5 min, and irradiation power of 640 W using the response surface methodology (RSM). Furthermore, the kinetic analysis of UE was investigated using three different empirical models. The chemical components of the essential oil extracted using each extraction method were identified as oxygenated monoterpenes, sesquiterpenes, and oxygenated sesquiterpenes using gas chromatography. Following extraction using various techniques, the morphology of spent leaves lost its distinct texture, their oil glands were entirely distorted, and their vascular bundles could still be identified. It was observed that the hydrogen bond interaction between the solvent molecule and 1,8-cineole-like value-added components played a role in the extraction. Among the investigated techniques, the solvent-free ME method is the most environmentally acceptable method and could effectively extract essential oil from *E. cinerea* leaves.

1. Introduction

Essential oils are produced from eucalyptus plants, which contain concentrated volatile fragrant components. Currently, there are approximately 700 different species of eucalyptus trees and bushes globally. Essential oils found in eucalyptus foliage is significant among wood or non-wood items. A range of monoterpenes, sesquiterpenes, oxides, ethers, alcohols, aldehydes, esters, ketones, and aromatic phenols makes up the majority of the constituents of essential oils.[1,2] Especially, 1,8-cineole compounds are present in large quantities in *Eucalyptus* oil and have potential for extensive application.[3,4] Owing to its

pharmacological properties, 1,8-cineole is a crucial chemical constituent with major medicinal value such as potent antioxidant, anti-microbial, anti-inflammatory, and anti-leishmanial properties.[5] Moreover, its medicinal and odoriferous properties are utilized in a wide range of products, including foods, medications, and chemicals. In addition, several studies revealed that 1,8-cineole is a superior bioactive substance and has a remarkable implication in dealing with cancers, digestive disorders, respiratory diseases, cardiovascular illness, dysphoria, bacilli, and Alzheimer's disease.[6,7]

However, there are limited reports on the main cineole molecules present in the essential oil of *Eucalyptus* species such as *Eucalyptus saligna*, *E. baueriana*, *E. cinerea*, *E. urophylla*, *E. viminalis*, *E. crebra*, *E. tereticornis*, *E. smithii*, *E. globulus*, *E. polybractea*, *E. benthamii*, *E. camaldulensis*, *E. maiden*, *E. astringens*, *E. sideroxylon*, *E. bicostata*, *E. melanophloia*, and *E. microtheca*.[8–10] Surbhi Kumar *et al.*[11] summarized the concentration of major bioactive components reported in various species of *Eucalyptus* such as *E. globulus* (72.71–85.5%), *E. camaldulensis* (8.7–74.7%), *E. loxophleba* (39.4%), *E. leucoxylon*

[a]Department of Chemical and Biomolecular Engineering, Chonnam National University, Yeosu, Jeonnam-59626, South Korea. E-mail: hsbyun@jnu.ac.kr

[b]Department of Chemical Engineering, Sri Venkateswara College of Engineering, Chennai-602117, India. E-mail: rgovind@svce.ac.in

[c]Department of Biomaterials, Saveetha Dental College and Hospitals, Saveetha Institute of Medical and Technical Sciences, Chennai-600077, India

(59.1%), *E. cinerea* (56.9–88.5%), *E. citriodora* (2.9–54.1%), *E. grandis* (18.4–19.8%), *E. saligna* (6.2–93.2%) and *E. tereticornis* (18.6–37.5%). Based on the quantity and strength, the extraction yield of 1,8-cineole varies using different extraction methods. Apart from this, the application of *Eucalyptus* species (bio-sorbent) was reported for the removal of toxic heavy metals of Pb, Cd, and Cr from the textile and leather industries.[12] Due to their broad biological and pharmacological properties, the extracted bioactive compounds are employed in the preparation of food, cosmetic formulations, and cleaning items; in addition, as a drug ingredient in liniments, expectorants, and inhalants. Surprisingly, Akhtar *et al.*[13] identified that 1,8-cineole acts as a potent inhibitor of COVID-19 infection through molecular-level bonding studies. In addition, 1,8-cineole possesses a high isobaric molar heat capacity of 300 Joules per mole per Kelvin at 25 °C and low vapor pressure, making it an eco-friendly thermic fluid and suitable for heat transfer applications.[14] Considering its numerous benefits, research has focused on the extraction of 1,8-cineole from *E. cinerea* foliage. Moreover, the *E. cinerea* species is selected based on its high-content oil yield; however, no research has been conducted to effectively enhance its oil yield. Hence, the *E. cinerea* species was employed in the present study to extract valuable products of 1,8-cineole.

Several conventional and modern methods have been reported for the extraction of essential oils from *Eucalyptus*. The conventional methods for the extraction of various essential oils are widely used on a commercial scale.[15,16] Alternatively, technological advancements have led to the development of new methods that can be valuable in certain situations, such as production and application. The most viable reported conventional and modern extraction methods are hydro-distillation (HD), Soxhlet extraction (SE), ultrasonication (UE), and microwave extraction (ME).[17–20] Among them, due to its high essential oil yield recovery and cost-effective equipment, the hydro-distillation method has been identified and used on an industrial scale. A distinct traditional method is Soxhlet extraction, where the solvent is circulated through the extractor multiple times. The Soxhlet extractor extracts the components using the condensed vapors of the solvent. However, the application of conventional SE techniques is frequently restricted by the mass transfer resistance resulting from multiple phases in the system. The duration of this separation process varies depending on the diffusion rates of the solvents. Additionally, because typical extraction methods operate at high temperatures, they consume a lot of energy and yield low-quality essential oil.[21,22]

As a result, modern ultrasound-assisted and microwave-assisted extraction techniques have been developed to enhance the quality and quantity of the bioactive components in all aspects.[23,24] UE and ME have attracted notable attention for the extraction of various value-added compounds from biomass sources in the last few years. Between them, UE is an environmentally friendly technique because it uses fewer solvents and chemical additives, requires less time, and facilitates easier separation and reusability of the components. Many authors have established that UE facilitates effective oil yield by varying processing factors such as the extraction time, power ratio, temperature, solid–solvent ratio (SSR), and pH of the mixture. However, there is the possibility that this method will make the extracted components less stable, and thus research is being done to address this issue. Meanwhile, ME techniques have attracted increasing attention for the extraction of essential oils. The two mechanisms responsible for microwave heating are ionic conduction and dipole rotation.[25] This technology is suitable for the extraction of polar and non-polar compounds. Several reports suggested that high-quality essential oil can be achieved by optimizing the process parameters such as irradiation power, extraction time, and solvent and solid ratio.[26] Studies have been devoted to adopting solid-state and solvent-free extraction techniques under microwave irradiation because of the increased focus on environmental preservation and clean technology. In this case, the obtained product has identical characteristics to that generated after 2 h of conventional HD, as described by Filly *et al.*,[27] although no solvent was employed. Alternatively, the response surface methodology (RSM) has been used to enhance the oil yield by optimizing the process parameters.[28,29] However, limited research articles have been published on the use of HD, SE, US, and ME for extracting 1,8-cineole from various species of *Eucalyptus* foliage. To the best of our knowledge, no reports have been published on the extraction of 1,8-cineole from *E. cinerea* foliage through different extraction techniques and a comparison of their performance. Furthermore, many studies did not explain the interaction mechanism and kinetic modelling of various extraction processes. Hence, considering all these shortcomings, the present study was formulated and conducted the corresponding research for the first time.

In this study, both conventional (HD and SE) and modern (UE and ME) methods were utilized to extract 1,8-cineole from *E. cinerea* leaves. The maximum oil yield was achieved by varying the process parameters such as foliage size, solid–solvent ratio, extraction time, temperature, sonication power, irradiation power pH, and ethanol–solvent ratio. Furthermore, RSM was applied to investigate the optimal conditions for UE and ME. Further, the performances of UE and ME were evaluated using different kinetic models. Finally, the interaction mechanism of the various types of extraction methods was elucidated.

2. Materials and methods

2.1. The profile and collection of plant material

Eucalyptus cinerea species belongs to the Myrtaceae family, typically growing to a height of 15–30 m. Its green leaves are glaucous and broadly egg-shaped to round (<80 mm long and <50 mm wide), and its fruits are 4–7 mm in size, woody and bell-shaped capsules. Its flowers are white and bloom between May and November. All parts of the *Eucalyptus* plant such as bark, seeds, flowers, leaves, and stems contain a fragrant and refreshing aroma of volatile and aromatic compounds. In addition, the extracted bioactive compounds from these parts play a crucial role in medicinal chemistry owing to their anti-bacterial, anti-cancer, antioxidant, and anti-inflammatory
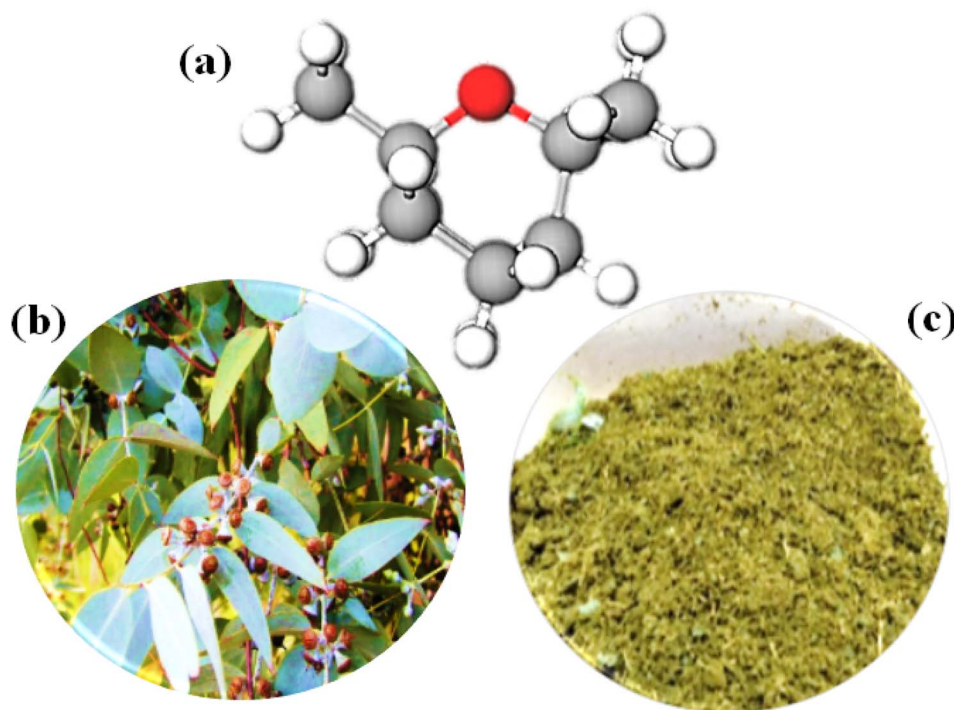
Fig. 1 Photographs of (a) the chemical structure of 1,8-cineole, (b) fresh *Eucalyptus cinerea* leaves, and (c) powdered plant leaves with a size of 2–5 cm.

properties. Hence, *Eucalyptus* inspired researchers to extract its essential oil. The essential oil yield of *E. cinerea* was reported to be 2.48–6.07%, consisting of several bioactive compounds such as 56.9–88.5% 1,8-cineole (*Eucalyptol*), 2–6.4% α-pinene, 5.9% limonene, 7.6% α-terpineol, 3.3% α-terpinolene, 4.8% terpinene-1-ol, 3.9% carvenone, and 11.2% *p*-cymene.[10,30] Among them, 1,8-cineole is a cyclic ether (Fig. 1a, $C_{10}H_{18}O$: 1,3,3-trimethyl-2-oxabicyclooctane) and has a high concentration, representing 40% oxygenated monoterpene components. This *Eucalyptol* compound has a spicy taste, camphor aroma and gives a fresh feeling.

The leaf samples were harvested for the study from mature *Eucalyptus* (*E. cinerea*) plants wildly grown in the nearby valley of Nellore region, Andhra Pradesh, India (14.43987°N latitude, 79.96917°E longitude) during January 2022 (Fig. 1b). The information of the species was identified and verified at Annamalai University (Department of Botany). The plant samples were rinsed with deionized water several times to eradicate foreign materials. Then, the leaves were air-dried under a shed until a consistent weight was achieved and stored at room temperature. The Karl Fischer method was used to quantify the moisture content in the air-dried foliage, which found to be 61% ± 0.1%.[31] Before the respective extraction, the leaves were ground with an electric grinder and powdered with an average particle size of 2–5 cm (Fig. 1c). The leaf and powder samples were stored in plastic zipper bags until processed.

All chemicals used were of analytical reagent grade. The test compound of 1,8-cineole (99%) was procured from Misri Fumet Pvt. Ltd, India. Deionized water was used to formulate all aqueous solutions during extraction.

2.2. Different techniques for essential oil extraction

This study investigated different extraction techniques, *i.e.* traditional (HD and SE) and contemporary (ME and UE) methods for extracting the bioactive compound of 1,8-cineole from *E. cinerea*.

2.2.1. Hydro-distillation. This approach involves heating a solution of water and the test material or other solvents to evaporate the bioactive chemical, and then liquifying the vapor in a condenser. The condensed aqueous phase is poured into a different container, where the water and essential oil is separated. In this study, the HD process was carried out in a Clevenger apparatus (Fig. S1a, ESI†) containing a 1000 mL round-bottom flask (30% reflux), and water was used as the solvent. A heating mantle was utilized to heat the apparatus with the sample set-up, and then the evaporated vapor was fed to the condenser where the glass receiver collected it. 100 g of 24 h dried foliage of *E. cinerea* was immersed in a 1000 mL flask with 500 mL of water solvent and distilled for 4 h. The SSR was maintained at 1 : 10 w/v (g mL^{-1}). Following the appearance of the first distillate drop in the receiver, the procedure was carried out for 5 h.[14] Essential oils were extracted using an extraction unit consisting of a flask of boiling solvent, required extracted part of the plant, condenser, and collection flask. The essential oil and the extraction solvent were collected in a receiving flask and separated by a separation funnel. The setup was kept overnight to allow it to cool and settle at room temperature. After this, a pinch of anhydrous sodium sulphate was added to the oil collected in a 15 mL centrifuge tube to remove the water on the oil (distillate). After isolation, the essential oil was kept at

−4 °C and used for further analysis. Initially, the impact of foliage size on the essential oil yield was investigated using two foliage sizes of 5 cm and 2 cm in length under two different SSRs of 1 : 25 and 1 : 10 g mL^{-1}. For the kinetic experiment, 5 cm and 2 cm foliage and 1 : 10 and 1 : 25 g mL^{-1} SSR were used for the HD extraction. The sample was collected at intervals of 30 min for 30, 60, 90, 120, 150, and 180 min and the pH was maintained at 7. All measurements were performed in duplicate. The yield of the collected essential oil (%) was calculated using eqn (1), as follows:

$$\text{Essential oil yield}(\%) = \frac{\text{mass of oil collected, g}}{\text{mass of dried plant material, g}} \times 100 \quad (1)$$

The quantity of 1,8-cineole in the extracted essential oil was analyzed using a GC-FID chromatogram. Eqn (2) was used to calculate the extraction yield of 1,8-cineole.

$$1,8\text{-Cineole yield}(\%) = \frac{\text{peak area of 1,8-cineole}}{\text{total peak area}} \times \frac{\text{essential oil yield}}{100} \quad (2)$$

where the peak area of 1,8-cineole refers to the area under the 1,8-cineole peak in the GC-FID chromatogram; the total peak area refers to the total area under all peaks in the GC-FID chromatogram; and the essential oil yield is the yield of essential oil extracted from the eucalyptus foliage (%). Finally, the 1,8-cineole yield was obtained at different intervals, and the data were fitted to obtain the extraction rate constant for the kinetic study.

2.2.2. Soxhlet extraction. A solid–liquid extraction technique was employed in the Soxhlet extractor to extract 1,8-cineole from *E. cinerea*. 100 g of dried foliage powder was kept in a thimble and placed in the Soxhlet chamber (Fig. S1b, ESI†). An appropriate quantity of solvent (ethanol) was added to the sample in a round-bottom flask connected to the Soxhlet extractor set-up for the distillation process. The solvent and essential oil were condensed using a thermal flask holding the solvents and a condenser fastened to the top of the Soxhlet extractor. Throughout the experiment, a heating mantle was used to heat the solution, and the temperature was recorded by a thermometer and maintained at 100 °C and the pH at 7. After the extraction, the solvent was extracted from the essential oil at 60 °C (10 kPa) using a rotary evaporator through liquid–liquid extraction.[32] The experiment was performed by taking four samples with varying solvent ratios of 1 : 05 g mL^{-1}, 1 : 10 g mL^{-1}, 1 : 15 g mL^{-1}, and 1 : 20 g mL^{-1} respectively, at a constant extraction time of 6 h. All measurements were performed in duplicate. Further, the experiment was conducted to estimate the effect of the extraction time on the yield of 1,8-cineole. The experiment was performed with ethanol as the solvent for different intervals ranging from 1 to 10 h at a constant SSR of 1 : 10 g mL^{-1}. Each set of extraction runs was conducted in duplicate. The essential oil yield was calculated using the mean extraction value and eqn (1) and the 1,8-cineole concentration was quantified using GC-FID analysis and its yield was calculated using eqn (2).

2.2.3. Ultrasound-assisted extraction. An ultrasonic homogenizer with a titanium probe and configurable sensor was used to perform the extraction. The sonicator (Sonics, 240 W, 40 kHz) produces an ultrasound effect in aqueous solution (Fig. S1c, ESI†). The temperature was detected using a temperature sensor inside the extraction set-up. The ultrasonic probe was immediately submerged in the sample-containing solvent. The effect of cavitation and bubble implosion aided the extraction process in the ultrasonic instrument. 100 g of eucalyptus foliage powder was fed into a 1000 mL beaker. The experiment was carried out by optimizing the sonication power by varying the power at 120, 200, 240, 320, and 400 W and keeping the other parameters constant such as solid and solvent ratio of 1 : 10 w/v (g mL^{-1}), extraction time of 15 min, pH of 5, ethanol–water ratio of 20 vol% and temperature of 60 °C. A glass vessel with a 1000 mL capacity was employed for the extraction and was stored in the extraction setup. A 10 mm diameter probe was used for sonication. A similar experiment was conducted to optimize the pH for maximizing the yield by varying the pH of the aqueous solution at 3, 4, 5, 6, and 7 with a constant ethanol–water ratio of 20 vol%. The pH was adjusted by adding 0.1% hydrochloric acid to the extraction solution during ultrasonication. In addition, the SSR was also optimized by varying it at 1 : 05, 1 : 15, 1 : 20, 1 : 25, 1 : 30, and 1 : 35 w/v with a constant extraction time of 15 min and sonication power of 240 W (20%).

Furthermore, the optimization study was performed using RSM in MINITAB to maximize the oil yield. In these experimental runs, the independent variables of ethanol–water ratio (20, 40, and 60 vol%), pH (2, 4, and 6), and extraction time (10, 40, and 70 min) were varied under the ultrasonication effect. The temperature was maintained at 60 °C. All measurements were performed in duplicate. Table 1 shows the RSM matrix designed for the UE experiment to isolate 1,8-cineole from *E. cinerea*. For the kinetic study, the UE experiment was carried out in a controlled environment (pH of 6, SSR of 1 : 10 w/v, power rating of 20%, and ethanol–water ratio of 20 vol%) at different

Table 1 RSM design matrix of the ultrasound-assisted extraction optimization experiment

S. No.	Ethanol–water ratio (%)	pH	Extraction time (min)	1,8-Cineole (%)	
				Actual	Predicted
1	60	2	70	32.99	31.52
2	20	2	70	6.80	7.01
3	60	2	10	1.01	2.35
4	40	4	40	11.92	15.23
5	40	4	40	11.81	15.23
6	60	6	70	11.96	12.65
7	60	6	10	1.21	3.42
8	20	6	10	52.31	58.65
9	40	4	40	14.36	15.23
10	40	4	40	10.56	15.23
11	40	4	40	18.31	15.23
12	**20**	**6**	**70**	**73.04**	**74.48**
13	40	4	40	12.16	15.23
14	20	2	10	3.20	5.0

intervals of 10, 30, 50, 70, and 90 min by varying the temperature at 60 °C and 45 °C. Three mathematical kinetic models were applied to infer the performance of the UE of 1,8-cineole. After each extraction run, the collected samples were filtered with Whatman filter paper (0.2 mm), and then fed into separating funnels (Fig. S1d, ESI†) to allow them to settle. The collected oil layer was subjected to centrifugation and stored at −20 °C until analysis.[33] GC-FID analysis was used to identify the quantity of 1,8-cineole content in the extracted essential oil.

2.2.4. Microwave-assisted extraction. The ME experiment in the microwave internal chamber required less extraction time and the solid–solvent ratio played a crucial role in extracting the maximum oil yield. During this method, the discharge of CO_2 was minimized to reduce its environmental impact. An appropriate amount of *E. cinerea* foliage powder was immersed in a 500 mL beaker with water solvent and kept in a domestic microwave oven (Fig. S1e, ESI†). Then, the heated mixture was taken out from the oven and the extract separated from the residue using Whatman filter paper (0.2 mm), which was fed into separating funnels to allow it to settle.[34] The moisture content was maintained at 61% given that ME can affect the moisture level of the foliage. Initially, pre-optimization studies were carried out for SSR, irradiation time, and microwave power. During the optimization of the SSR (2–7 g mL^{-1}), the other parameters were kept constant such as extraction time of 3 min and power of 480 W. The irradiation time was varied from 3 to 6 min to optimize the irradiation time, while keeping the SSR (3 g mL^{-1}) and power (480 W) constant. Furthermore, the microwave power was optimized by varying the power from 160–800 W at a fixed SSR and extraction time.

The RSM optimization study was carried out by varying the irradiation power level (160–800 W), extraction time (1–10 min), and SSR (2–10 g mL^{-1}) to maximize the extraction yield of 1,8-cineole. The extraction experiments were investigated at pH 7 and temperature of 45 °C. Table 2 shows the RSM design matrix developed for the microwave-assisted extraction using the MINITAB software. The collected oil layer was subjected to centrifugation and stored at −20 °C for further analysis. Each

run was analyzed using GC-FID to calculate the yield of 1,8-cineole. All measurements were performed in duplicate.

2.3. Analytical methods

Gas chromatographic analysis was done to quantify the concentration of 1,8-cineole in the extracted essential oil. The oil sample obtained from various methods including HD, SE, UE, and ME was characterized using a gas chromatograph (GC Model: HP5890; Hewlett-Packard, USA) equipped with a flame ionization detector (FID). A BP-1 (HP) capillary column with the dimensions of 30 m × 0.25 mm was used for the analysis. The chromatogram was recorded under the following operating conditions: H_2 carrier gas at a flow rate of 2 mL min^{-1}, 1/50 split mode, oil sample injection volume of 1 µL, injector and detector temperature of 250 °C, and for the column, a temperature gradient was used, starting at 60 °C and increasing by 3 °C at one minute intervals until the temperature reached 220 °C. The samples were diluted to 0.5% (v/v) in chloroform. The standard calibration curve ($R^2 = 0.9990$) was used to calculate the area %, and hence determine the quantity of 1,8-cineole. The areas of the cineole peaks in each extract were compared to that of the two internal standards injected twice.

Scanning electron microscopy analysis (SEM) was performed for the powdered *E. cinerea* foliage before and after ME. The adaxial and abaxial foliage surface was analyzed before and after extraction. The overlying cells covering the area of the secretory cavities were also investigated. The morphological changes in the inner cuticles of the leaf were examined before and after extraction. Importantly, the structural characteristics of the extracted residues from each extraction method for different process conditions were analyzed. The inside and outside lateral surfaces, isolated cuticles, and residues obtained after extraction were examined using an SEM analyzer (Philips XL30, USA). The dried foliage powder/essential oil was mixed in 2.5% glutaraldehyde and 4% formaldehyde to prepare the specimen. After that, it was dried in an oven for 6 h, rinsed in ice-cold phosphate buffer at pH 7.2, and left overnight. Subsequently, the sample was coated with carbon, and then subjected to SEM analysis to record SEM images and determine its thickness, with 10–20 repetitions. The GC and SEM analyses were performed at Tamil Nadu Test House, Vanagaram, India.

2.4. Statistical analysis

Regarding the RSM experimental design and analysis, MINITAB software version 17 was used for statistical analysis. The findings of the preliminary single-factor analysis in the UE and ME process were the basis for using the full-factorial randomized experimental design.

3. Results and discussion

E. cinerea is a medicinal plant with a high concentration of bioactive compounds sequestered in its leaves, which can be used to produce essential oil, adding further value. Various extraction techniques produce different yields; however, to enhance the extraction yield, the appropriate extraction method

Table 2 RSM design matrix of the microwave-assisted extraction optimization experiment

S. No	Solid–solvent ratio (g mL^{-1})	Extraction time (min)	Irradiation power (W)	1,8-Cineole (%) Actual	1,8-Cineole (%) Predicted
1	5	5.5	160	39.77	40.23
2	5	5.5	480	44.04	49.85
3	5	5.5	640	76.43	75.05
4	2	1	800	45.42	48.98
5	8	1	160	50.30	59.53
6	8	10	160	58.32	56.85
7	5	5.5	480	39.08	49.85
8	2	10	160	29.06	29.56
9	10	5.5	480	42.95	40.52
10	8	10	800	18.33	17.63
11	**2**	**4.5**	**640**	**95.00**	**95.62**
12	5	3	480	58.94	57.02
13	8	1	800	33.45	36.74

is required. In this section, we discuss the results from various extraction strategies for 1,8-cineole and their kinetic studies.

3.1. Hydro-distillation extraction technique

The essential oil extracted from *E. cinerea* by HD contained volatile compounds, which were comprised of free volatile and glycoside-bound volatile compounds. Approximately 10 times more free volatile oil (3.1%) was obtained from the *E. cinerea* foliage than bound volatile oil (0.4%) during hydro-distillation. It was observed that the free volatile content in the oil was found in the major fractions and could be produced by HD extraction. Especially, the bioactive compound of 1,8-cineole was accumulated highly in the free volatile oils.[6] Mann *et al.*[30] investigated the free volatile and bound volatile compounds during the HD extraction of *E. cinerea*. These authors identified that the major fractions in the free volatile oil were β-pinene, myrcene, limonene, 1,8-cineole, *p*-cymene, *trans*-pinocarveol, δ-terpineol, and globulol exhibited. Alternatively, α-terpinene, γ-terpinene, terpinen-1-ol, carvenone, α-terpinolene, iso-terpinolene, *p*-cymenene, iso-amylalcohol, borneol, neoisopulegol, camphene, *cis*-3-hexen-1-ol and 3,8-*p*-menthadiene were accumulated in the glycoside-bound volatile oil. Hence, HD has the potential for extracting 1,8-cineole from *Eucalyptus*; however, no reports have shown the impact of foliage size on the essential oil yield.

3.1.1. Effect of size of foliage on oil yield during hydro-distillation. The size of the *E. cinerea* foliage has an effect on the extraction yield of 1,8-cineole. This azeotropic (water–oil) distillation is conducted by the action of internal diffusion and desorption of the substrate. The size of the *E. cinerea* leaves played a significant role in the diffusion, followed by the extraction of oil glands. Thus, to study the size effect, two sizes of 5 and 2 cm long were investigated under two different SSRs of $1:25$ and $1:10$ g mL^{-1} in the HD unit. Hence, four runs were conducted to calculate the % yield of 1,8-cineole. Fig. 2a and b show the effect of the size of the leaves and SSR on the yield of essential oil (1,8-cineole), respectively. The essential oil yield increased from 1.5 to 3.5 mL (16–37%) when the size of the foliage decreased from 5 cm to 2 cm. On the contrary, the oil yield was reduced when the SSR increased from $1:10$ to $1:25$ g mL^{-1}. It was observed that the maximum concentration of 1,8-cineole (72.151%) was obtained for small-size leaves (2 cm) under the minimum SSR ($1:10$ g mL^{-1}) within a short period (4 h). This is because the smaller size particles enhanced the diffusion, *i.e.* mass transfer rate. Typically, the grinding of leaves reduces the particle size, resulting in an increased superficial area, and exposes essential oil-bearing structures within the foliage. Consequently, the disruption in the cell wall facilitates the solubility and effective extraction of bioactive compounds within a shorter extraction time.[35] Furthermore, grinding to a smaller foliage particle size contributes to a smaller diffusion distance and larger diffusion area, thereby increasing the mass transfer rate and extraction rate at the minimum extraction time. Thus, smaller particles support enhanced diffusivity, and the increased mass transfer rate constant results in readily extractable phenolic compounds from grounded foliage.

An increase in temperature also significantly enhanced the extraction of oil glands during distillation; hence, it follows first-order chemical kinetics. The percentage of 1,8-cineole was reduced for the big-sized eucalyptus foliage due to the mass transfer limitation between the solvent and solid. Tesfaye and Tefera[32] revealed that minimizing the solid size with an increase in temperature significantly enhances oil extraction. At elevated temperatures, the diffusion rate and evaporation rate increased, contributing to more contact duration for the solvent and plant source.[36] Thus, we inferred that the reduced size of the leaves contributed to increased contact with solid leaves containing oil. Increasing the mass transfer rate enhanced the extraction rate, maximizing the oil yield, followed by high phenolic compound extraction. The negative effects of the high solvent volume include dilution of the essential oil, increased solvent retention, longer distillation time, which contributes to the degradation of the essential oil and increased energy consumption, reduced vapor pressure, leading to slower essential oil release, and over-extraction, leading to the extraction of undesirable compounds, thus affecting the quality of the essential oil.[37] In the case of a higher water content, the heat could be wasted in heating the water and the hydrolytic effect may have contributed to reducing the extraction process efficiency and lowering oil yield. Further, a high solvent volume shifted the equilibrium, hindering the diffusion and mass transfer of the phenolic components.[38] Thus, excessive solvent lowered the extraction selectivity for the target compound. The effective procedure using the HD method for extracting essential oil from leaves makes it easy to use both on a small and large scale and free of chemicals.[39] Hence, the HD method is a potential method to extract the maximum yield of 1,8-cineol from *E. cinerea* leaves.

3.1.2. Kinetic modeling of hydro-distillation. It is commonly known that a significant portion of the free volatile oil found on the outside, inner pores, or uniformly distributed throughout the glands are extractable oil components. Mathematical models are widely used to correlate the kinetic behavior of plant materials with the location of free volatile oil in HD. Researchers have found that most of the oil is accumulated in the exogenous glands, which follows the first-order kinetic model based on certain assumptions.[40] During hydro-distillation, the rate of evaporation is dependent on the solubility of the components, and hence the extraction process is assumed to be a mass transfer rate process. Hence, this method uses the first-order kinetic equation, where the amount of oil removed each time is directly proportional to the amount accumulated in the foliage. As the distillation proceeds, the oil concentration decreases, hence the simplified kinetic eqn (3) applies, as follows:

$$\ln \frac{1}{1-y} = kt \qquad (3)$$

where 'y' represents the fraction of oil distilled, 'k' is the first-order rate constant (min^{-1}), and 't' is the extraction time (min). To authenticate the kinetic model, a graph was plotted of $\ln(1/1-y)$ *vs.* t for the experimental data conducted at different intervals from 30 to 180 min. Fig. 2c shows the graphical
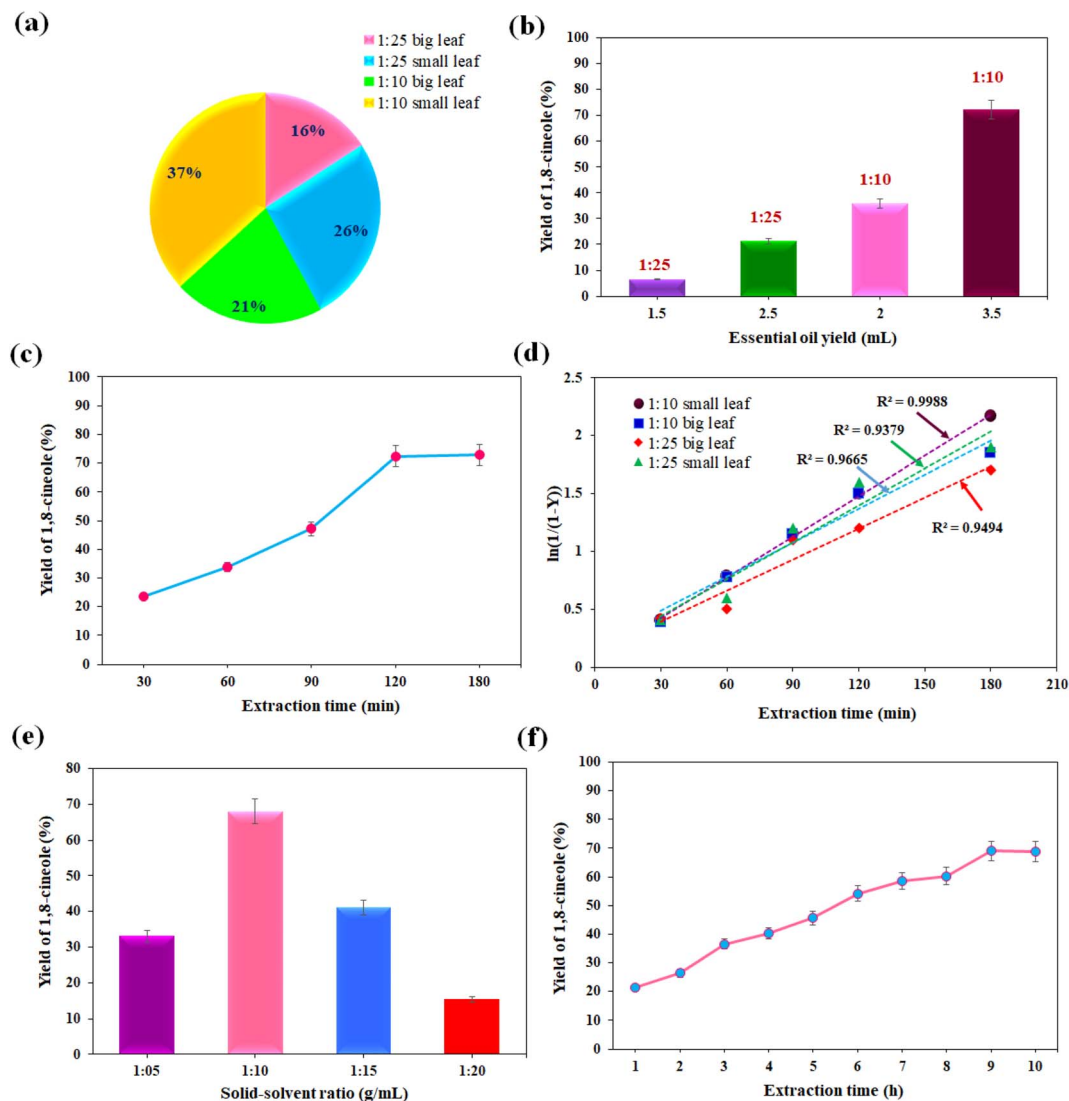
Fig. 2 Graphical representation of the (a) effect of the size of the leaves on the yield of essential oil in HD, (b) effect of the solid–solvent ratio on the yield of essential oil in HD, (c) effect of extraction time on the yield of 1,8-cineole in HD, (d) first-order kinetic model for the HD extraction process of different leaf sizes together with various solid–solvent ratios, (e) effect of solid–solvent ratio on the yield of 1,8-cineole in SE, and (f) effect of extraction time on the yield of 1,8-cineole in SE.

representation of the effect of extraction time for HD on 1,8-cineole yield. The yield of eucalyptol increased (72.85%) with an increase in the extraction time up to 180 min.[41] The first-order extraction kinetics were plotted as $\ln(1/(1 - y))$ vs. t and presented in Fig. 2d. The kinetic data for all four different samples with varying leaf sizes and SSR was presented, and the results are as follows: (i) $1:10$ g mL^{-1} small leaves with an R^2 value of 0.9988 and an extraction rate constant of $K = 0.0131$ min^{-1}, (ii) $1:10$ g mL^{-1} big leaves with an R^2 value of 0.9665 and an extraction rate constant of $K = 0.0115$ min^{-1}, (iii) $1:25$ g mL^{-1} small leaves with an R^2 value of 0.9379 and an extraction rate constant of $K = 0.0098$ min^{-1}, and (iv) $1:25$ g mL^{-1} big leaves with an R^2 value of 0.9494 and an extraction rate constant of $K = 0.009$ min^{-1}. According to the graph, it was inferred that the experimental data for the small leaf with $1:10$ g mL^{-1} SSR run strongly fits the first-order kinetics with the maximum

extraction rate constant ($K = 0.0131$ min^{-1}). The larger rate constant value obtained using smaller (2 cm) foliage with $1:10$ g mL^{-1} SSR indicates an increased driving force, resulting in faster diffusion or mass transfer. Therefore, using small foliage is ideal to get a higher oil yield in a relatively short duration of distillation. Further, the plot yielded a straight line, and hence the HD follows the first-order kinetic model, and this trend is consistent with the findings elucidated by Samadi *et al.*[42] who used *Aquilaria malaccensis* leaves to extract essential oil. It was observed that the oil content in the glandular trichomes or epidermal hairs is freely available, making it easy to extract. As a result, there is negligible resistance to mass transfer during distillation, which helps achieve fast equilibrium between the phases.[14,43] Thus, the smaller particle size leads to improved mass transfer and quickly extracts the oil content from the foliage.

3.2. Impact of processing variables on oil yield during Soxhlet extraction

The experiment on the impact of SSR and extraction time on the 1,8-cineole yield during SE was investigated, and the findings are illustrated in Fig. 2e and f, respectively. The experiment were performed in triplicate and error bars were predicted through standard deviation calculations. The yield of 1,8-cineole increased (68.07%) up to the SSR of 1 : 10 g mL^{-1}, and then decreased with an increase in the ratio to 1.20 g mL^{-1}. It was noted that the maximum amount of 1,8-cineole was extracted at the minimum SSR at a temperature of 100 °C. In the case of the optimum SSR, a solvent volume of 10 mL was found to be the required amount for enhancing the diffusion rate and maximizing the solubility of phenolic compounds during the SE process. Further, an increase in the volume of ethanol solvent denaturalized the bio-active target compound and a longer time was necessary to improve the essential oil yield. The impact of extraction time on the yield of 1,8-cineole was shown in Fig. 2f. The obtained 1,8-cineole yield increased from 26.35% to 69.01% with an increase in the extraction time from 1 to 9 h. Thus, the maximum yield of essential oil and 1,8-cineole was 35.39% and 69.01% at 9 h, respectively. Also, an increase in the extraction time effectively ruptured the cell walls and oil glands and increased the exposure of the solvent to the foliage, enhancing the extraction of the essential oil. In this case, an extraction time of 9 h led to an adequate contact time between the solvent and foliage, resulting in an improved oil yield. However, a longer (>9 h) extraction time contributed to the degradation of the phenolic compounds, which reduced the target compound 1,8-cineole yield. Further, the oil yield remained stable at 9 h when the equilibrium time was reached in response to an increase in extraction time. It was observed that the 1,8-cineole yield rapidly increased to 69.01% at 9 h, indicating that the equilibrium time was reached, and no further extraction was observed in the SE process. Hence, the optimized SSR for the SE of eucalyptol was identified to be 1 : 10 g mL^{-1}, and the maximum 1,8-cineole yield was found to be 69.01% at 9 h. The extraction of essential oil from plant leaves depends largely on the usage of an ideal solvent.

Zhao and Zhang[41] revealed that the percentage of 1,8-cineole yield was the maximum when ethanol was used as the solvent (36.33% at 8 h) and the yield was minimum when using hexane as the solvent (7.90%) for the SE of oil from *Eucalyptus loxophleba*. The obtained 1,8-cineole concentration in this study is higher than the reported concentration. This is due to the different *Eucalyptus* species used in our study. Furthermore, ethanol is a strong polar solvent, and hence it extracts many polar compounds that contain O–H bonds such as 1,8-cineole, cadinene, carvone, myrtenol, tetradecanoic acid, 1,2,3-benzenetriol, and sitosterol. The components readily interacted with the hydrogen bond of ethanol and separated easily during SE. Hence, the use of ethanol solvent in the SE method is an ideal strategy for extracting the maximum quantity of 1,8-cineole.[44] When comparing the results of SE with ethanol, *E. cinerea* leaves have a different potential polar compound than *E. camaldulensis* and *E. globulus* leaves.[45]

3.3. Total extraction yield of ultrasound-assisted extraction

3.3.1. Effect of sonication power, pH, and solid–solvent ratio on oil yield. The operating conditions have a significant impact on the outcome of ultrasonic extractions. Many studies have confirmed that the extraction process factors of sonication power, extraction time, pH, temperature, solvent-solid ratio, and % of ethanol in water influence the oil yield from different plant sources.[33,46] During the pre-optimization study, the impact of sonication power, pH, and SSR on the yield of 1,8-cineole was investigated for the extraction time of 15 min, ethanol–water ratio of 20 v%, and temperature of 60 °C. The results obtained from the optimization of sonication power showed (Fig. 3a) that an increase in sonication power from 120 to 400 W generally favored an increase in the oil yield. With a further increase in the power from 240 to 400 W, the yield was significantly reduced, and the maximum yield was found to be 49.56%. During ultrasonication, the generation of acoustic cavitation bubbles increases the mass transfer rate between the phases, increasing the surface contact area, which contributes to the rapid release of many value-added compounds and cell wall rupture in the plant material.

The acoustic cavitation mechanism involves two steps, the formation of microbubbles and subsequent collapse of the bubbles. Ultrasonic waves create microbubbles in the solvent during ultrasonication, which implode, releasing energy and creating high-temperature and pressure gradients, liquid jet turbulence, and increased mass transfer coefficient.[47] Typically, the gas–liquid interface plays a crucial role in essential oil release, where acoustic cavitation disrupts the *E. cinerea* leaf cell wall, releasing oil into the surrounding solvent of ethanol; mass transfer enhancement, where the gas–liquid interface increases the surface area for essential oil transfer from the foliage cells to ethanol; and solvent penetration, where the liquid jets and turbulence facilitate the entry of ethanol into the leaf cells, enhancing the extraction of 1,8-cineole.[48] The polarity of ethanol, formation of hydrogen bonds with essential oil components, and their low surface tension improve the penetration of ethanol into the foliage cells to increase the essential oil yield. An enhancement in the oil yield was observed by decreasing the extraction time surprisingly. Moreover, the *E. cinerea* leaves have many free volatile compounds, which contribute to high oil extraction with the support of the ultrasonication effect in the aqueous solution.

Further, the solid loading in the solvent was optimized at different ratios during UE, as presented in Fig. 3b When the SSR increased from 1 : 05 to 1 : 35 w/v, the extraction yield increased up to the ratio of 1 : 10 w/v, and then decreased with a further increase in the SSR. The maximum 1,8-cineole yield was 51.35% at an SSR of 1 : 10 w/v. The high volume of ethanol–water solvent affected the extraction yield and reduced the concentration of oil. When the solid loading in the experiment increased, maintaining the sonication time and ultrasound power in the experiment was not enough to extract a higher oil yield given that less solvent is required for the maximum sonication power used in this study. Fig. 3c shows the effect of pH on the essential oil yield. Upon optimization of the pH, it was found that the 1,8-
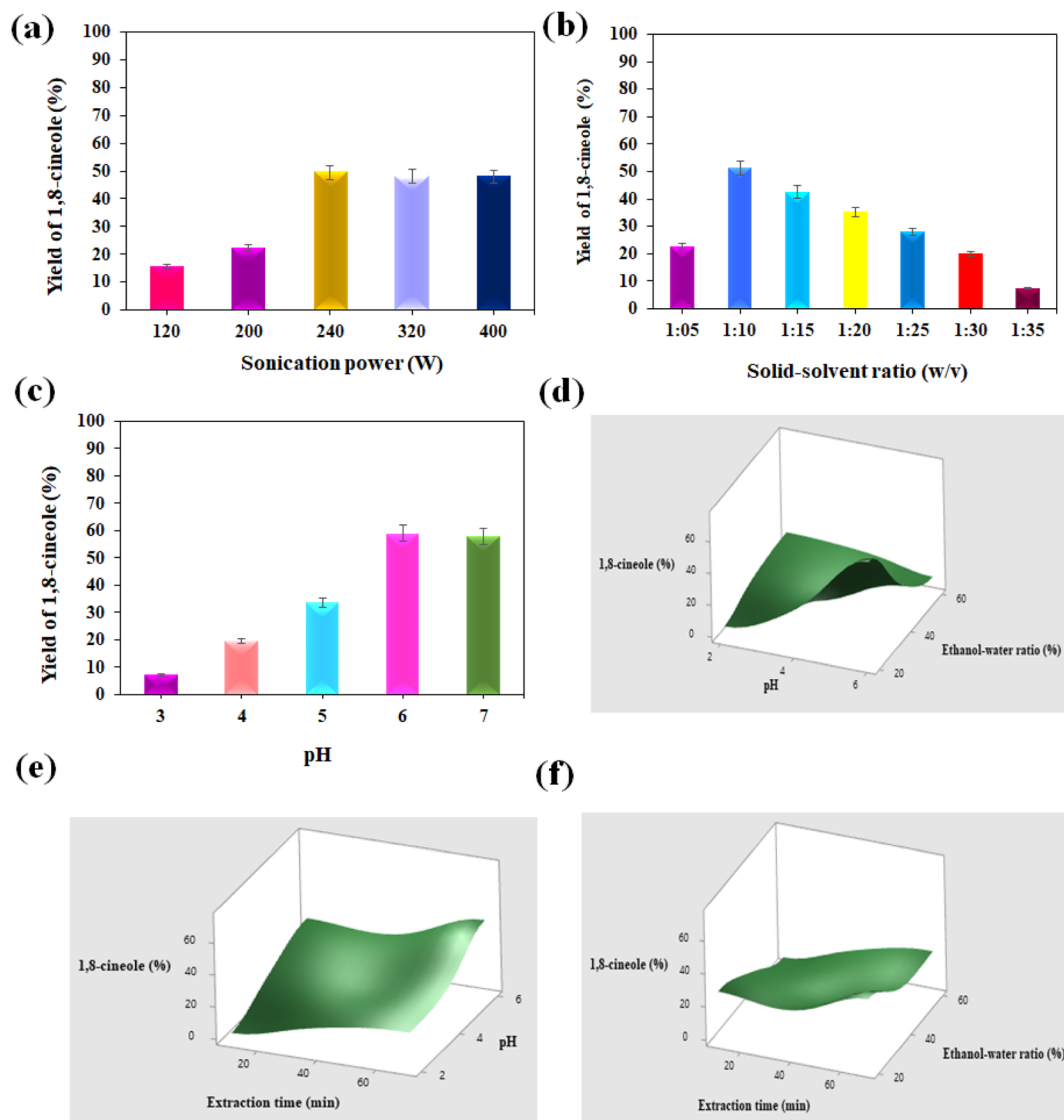
Fig. 3 Graphical representation of the (a) effect of sonication power on the yield of 1,8-cineole in UE, (b) effect of the solid–solvent ratio on the yield of 1,8-cineole in UE, (c) effect of pH on the yield of 1,8-cineole in UE, (d) interaction response effects of the ethanol–water ratio and pH, (e) interaction response effects of pH and extraction time, and (f) interaction response effects of the ethanol–water ratio and extraction time.

cineole yield decreased with an increase in the pH value from 6 to 7, and the maximum yield of 59.02% was observed at pH 6. The extraction yield of value-added compounds was improved under acidic conditions, whereas high pH values affected the extraction process, and subsequently reduced the 1,8-cineole yield. The addition of 0.1% HCl enhanced the foliage cell wall breakdown, releasing more essential oil components, and thereby increasing the solubility of the essential oil components. Notably, acidic pH increased the solubility of 1,8-cineole in ethanol and facilitated the release of more 1,8-cineole from plant materials during ultrasonication due to its stability and hydrolysis. Hence, acidic pH may favor the extraction of essential oil compounds, resulting in 1,8-cineole remaining stable at pH 2–7, whereas 1,8-cineole degrades at pH > 7. It was observed that the phenolic compounds in the plant source were extracted better at a pH value of 6. This method is economically

viable given that we achieved the maximum oil yield at the minimum operating conditions in the extraction process.

3.3.2. Effect of dependent variable response surfaces. Table 1 presents the design matrix for the performance of the UE method to enhance the oil yield from *E. cinerea* using RSM by varying the independent variables between the normalized values from −1 to +1. The response surface model was designed using independent variables to determine the optimal conditions for the extraction process. The matrix of 14 runs was conducted under different operating conditions with constant variables of ultrasound power (240 W), temperature (60 °C), and SSR (1 : 10 w/v). These independent variables showed obvious effects on the yield of 1,8-cineole. Three factors (ethanol–water ratio, pH, and extraction time) were further optimized to confirm the optimal levels using RSM design to achieve the maximum oil yield. Among the 14 runs, experiment 12

(ethanol–water ratio: 20 vol%, pH: 6, and extraction time: 70 min) produced the highest 1,8-cineole yield of 74.48%. The lowest yield of 1.01% was observed at pH 2, 60% ethanol in water and 10 min extraction time. The design model equation was used to predict the yield of 1,8-cineole from *E. cinerea* for the UE method.

Fig. 3d–f show the effects of the independent variable interactions such as ethanol–water ratio *vs.* pH, pH *vs.* extraction time, and ethanol–water ratio *vs.* extraction time, respectively, on the oil yield. According to Fig. 3d, the oil yield increased with a higher pH and lower volume of ethanol in water. Fig. 3e shows that the oil yield increased with an increase in the pH and extraction time. Fig. 3f indicates that the 1,8-cineole yield was affected when decreasing the extraction time and increasing the ethanol–water ratio. It was observed that a maximum 1,8-cineole yield was observed with increasing extraction time and pH and reducing the ethanol volume % in water. Hence, the maximum extraction of 1,8-cineole yield was achieved at a pH of 6, ethanol–solvent ratio of 20 vol%, and extraction time of 70 min. Thus, pH and extraction time have a positive effect, whereas the ethanol–solvent ratio negatively impacts the oil yield. There was an interdependence between pH and ethanol–solvent ratio given that for high pH values, the free volatile phenol contents were easily extracted with a low % ethanol–water ratio. In addition, the –OH groups of phenolic compounds dissociated well at high pH, contributing to the polarity of the components and making them easily soluble in water.[49] Gullón *et al.*[50] revealed that the hydroalcoholic condition favors the solubility of phenolic compounds, while 1,8-cineole, being more hydrophilic, facilitates extraction. A contradictory effect was observed for low pH with a high % of ethanol in the extraction solution.

Alternatively, there was an interdependence between extraction time and % ethanol in water. The ultrasonication time has a positive effect on the extraction with less % of ethanol in water. Nonetheless, the extraction time could be reduced with a slight increase in the ethanol %. The balance between the extraction and degradation processes could explain this. To maximize the yield of 1,8-cineole from *E. cinerea*, high pH, extraction time, and ethanol percentage in water were advised. Some authors reported the same behavior for varying pH, extraction time, and ethanol–water ratio for oil from different biomass sources.[24,51] In this method, the ultrasonication effect induces the cavitation effect with a bubble implosion effect, which is responsible for the enhanced performance of the UE strategy. In addition, ethanol does not degrade the phenolic compounds and favors the extraction of the maximum quantity of bioactive compounds from *E. cinerea*.

3.3.3. Kinetic studies of 1,8-cineole extraction for ultrasonication. To extend this study, three kinetic models were applied to model the 1,8-cineole extraction performance during UE. The extraction experiment was conducted at different temperatures (27 °C, 45 °C, and 60 °C) at extraction times between 10 and 90 min under a controlled environment (SSR of 1 : 10 w/v, pH of 6, power rating of 20%, and ethanol–water ratio of 20 vol%). Fig. 4a shows the effect of concentration of 1,8-cineole as a function of extraction time at temperatures of 60 °C,

45 °C, and 27 °C, respectively. At 60 °C, the concentration of eucalyptol initially increased with an increase in the extraction time up to 50 min, and then it started to decrease, as illustrated in Fig. 4a. The maximum extraction yield of 73.08% was observed at 50 min. Similarly, at 45 °C, the concentration of eucalyptol increased with an increase in the extraction time up to 50 min, and then decreased, as illustrated in Fig. 4a. The maximum extraction yield of 88.41% was observed at 50 min. At 27 °C, the concentration of eucalyptol increased with an increase in the extraction time up to 50 min, and then decreased, as illustrated in Fig. 4a. The maximum extraction yield of 34.81% was observed at 50 min. It was observed that the high temperature may cause the degradation of thermolabile compounds such as phenolic compounds.[51,52]

Palma *et al.*[33] identified that a temperature of above 70 °C may degrade the oil components during extraction. However, a temperature below 45 °C benefits the extraction efficiency of 1,8-cineole because of the increase in acoustic cavitation induced by the release of several value-added compounds at high concentration. Among the three temperatures, 45 °C was sufficient to extract 1,8-cineole from *E. cinerea* at 50 min. Hence, we conclude that medium temperature, high pH, low ethanol–water ratio, low SSR, medium sonication power, and high extraction time are recommended for extracting 1,8-cineole from *E. cinerea*. A lower solvent volume is sufficient for improved mass transfer due to the acoustic cavitation mechanism, which accelerates solvent–oil interactions thereby releasing essential oils more efficiently. The ultrasonic waves facilitate the deeper entry of the solvent into the plant cells with the minimum solvent volume (20 vol%). Three models were examined utilizing the linearized equations of the empirical models to comprehend the kinetics of the extraction data at 45 °C and 60 °C. Using the Microsoft Excel software, linear regression was performed to determine the model parameters. The extraction yield was evaluated according to the pseudo-first-order kinetics, as follows:[53]

$$\log Y = -k_1 t + \log Y_1 \tag{4}$$

where Y is the 1,8-cineole yield (%), t is time (min), k_1 refers to the extraction rate constant for diffusion (min^{-1}) and Y_1 is the extraction yield at saturation. Fig. 4b and c show the graphical representation of the kinetic model evaluated at 60 °C and 45 °C, respectively. The linear behavior was observed at the time of extraction. At 60 °C and 45 °C, they the maximum correlation of R^2 0.984 and 0.981 was achieved, respectively. The extraction rate constant for diffusion was determined to be 0.0183 and 0.0334 and the extraction yield at saturation was found to be 69.571 and 87.8835, respectively.

The solid–liquid extraction procedure was explained by the model created by Peleg for the description of sorption curves.[54]

$$C(t) = C(0) + \frac{t}{K_1} + K_2 t \tag{5}$$

where 'K_1' is Peleg's rate constant (extraction rate at the beginning of the extraction process, min^{-1}), 'K_2' is Peleg's capacity constant (maximum extraction yield over the extraction
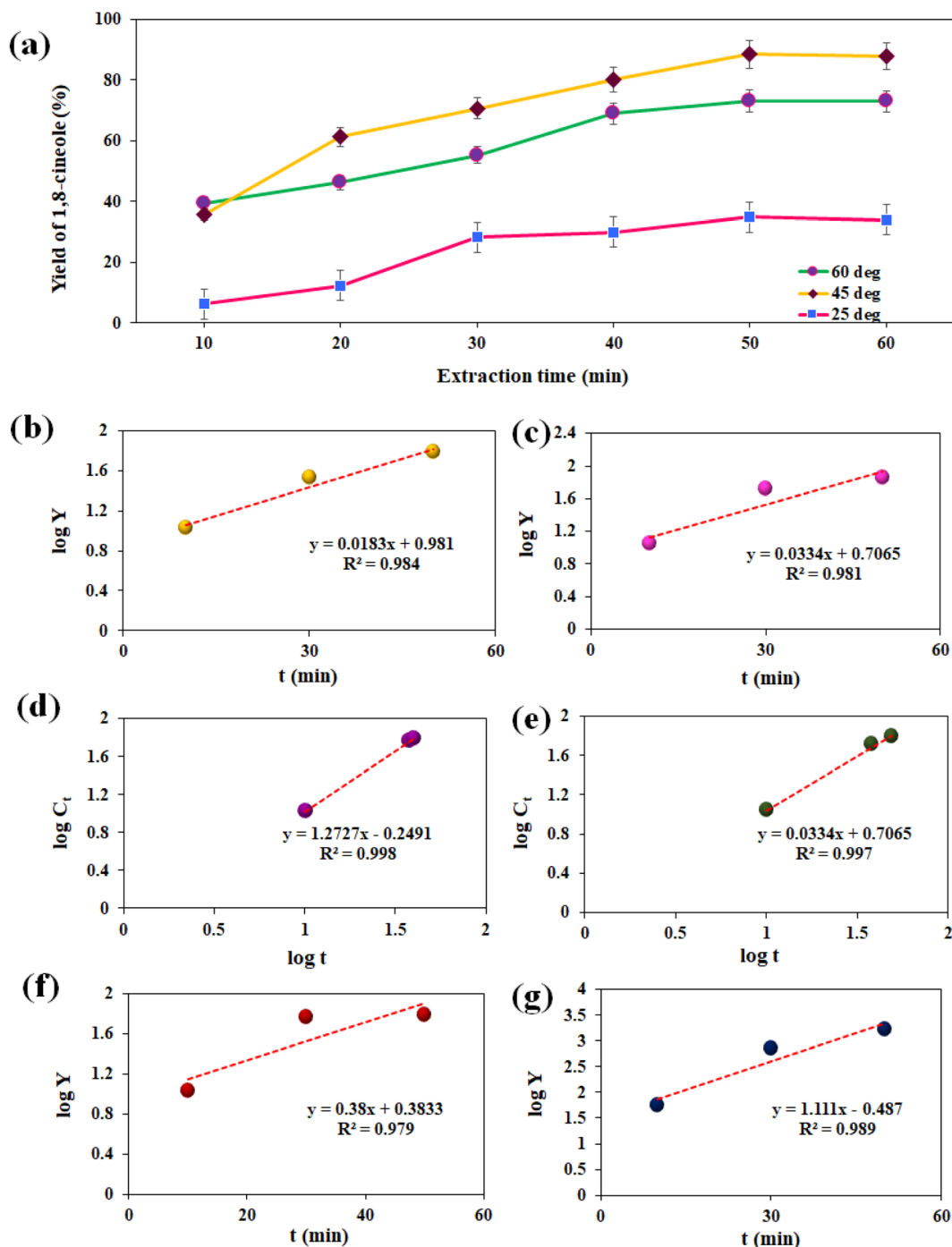
Fig. 4 (a) Effect of temperature and extraction time on the yield of 1,8-cineol in UE. Graphical representation of (b) pseudo-first-order kinetic model evaluated at 60 °C, (c) pseudo-first-order kinetic model evaluated at 45 °C, (d) Peleg's kinetic model evaluated at 60 °C, (e) Peleg's kinetic model evaluated at 45 °C, (f) power law model evaluated at 60 °C, and (g) power law model evaluated at 45 °C.

process), and $C(0)$ is the concentration of extraction yield at time $t = 0$ (hence $C(0)$ is zero). $C(t)$ reflects the concentration extraction yield at time 't' (final, $t = t$). Fig. 4d and e show a graphical representation of the kinetic model evaluated at 60 °C and 45 °C, respectively. Linear behavior was observed at the time of extraction. At 60 °C and 45 °C, the maximum correlation of R^2 0.998 and 0.997 was achieved, respectively. Peleg's rate constant was determined to be 0.053 min^{-1} and 1.186 min^{-1}

and Peleg's capacity constant was found to be 1.775 and 0.819, respectively.

Another useful empirical formula for solid–liquid extraction is the power law model, which can be expressed as follows:[55]

$$Y = Kt^n \qquad (6)$$

where n refers to the exponent of diffusion, indicating the transport mechanism, K is an extraction rate constant (carrier-

active agent, min^{-1}), 'Y' is the yield of 1,8-cineole (%) and t is time (min). The linearized equation becomes:

$$\log Y = n \log t + \log K \qquad (7)$$

Fig. 4f and g present a graphical representation of the kinetic model evaluated at 60 °C and 45 °C, respectively. Linear behavior was observed at the time of extraction. The maximum correlation of R^2 0.979 and 0.989 was achieved at 60 °C and 45 °C, respectively. The extraction rate constant was 2.398 min^{-1} and 0.908 min^{-1} and the diffusional exponent was 0.4 and 0.5, respectively. According to the results of the three models, the yield of 1,8-cineole has the same relation with the extraction time for the UE method. The kinetic constants at different temperatures were estimated using the slope and intercept values of the linear plot, as tabulated in Table 3. According to the results, we infer that the highest extraction rate occurs at lower temperatures, providing a higher 1,8-cineole content. According to the calculated R^2 values, the predicted model is in good agreement with the experimental results and these models are more suitable for evaluating the performance of biomass component extraction. However, among the models, the Peleg law model is the most accurate.

3.4. Total extraction yield of microwave-assisted extraction

Given that microwave technology is well-established and widely used in industry, it has an edge over other technologies and is frequently recommended as a green extraction method.[56] The internal heating of the water in the moisture-conditioned samples during the microwave extraction process caused the plant cells to swell, and eventually their oil glands burst.[53,57] This method improves the extraction efficiency and lowers costs by consuming less time and water. In this work, 1,8-cineole was extracted from the leaf of *E. cinerea* using ME.

3.4.1. Effect of solid–solvent ratio, irradiation power, and extraction time on oil yield. The single-factor pre-optimization studies optimized the extraction process conditions for the effective extraction of 1,8-cineole. Wei *et al.*[58] identified the optimum moisture content for extracting essential oil from *Cinnamomum longepaniculatum* leaves. They confirmed that a moisture content in the range of 54–74% favored the microwave extraction and increased the 1,8-cineole yield to the higher end. The lower the water content, the more likely the bottom raw materials are to gelatinize and hinder effective extraction. In contrast, the higher the water content, the more likely the surface of the leaves would adhere to other leaves, creating an interaction force between the water and the leaves particles, which make them stick together during the experiment and prevent stable extraction. Therefore, the moisture content of the *E. cinerea* leaves was maintained at 61% in the present study. During the investigation of the SSR impact, the yield of 1,8-cineole increased when the ratio increased to 3, and then it decreased with a further increase in the ratio (Fig. 5a). The maximum extraction yield was found to be 90.15% at 3 g mL^{-1} of SSR. When the solid content in water increased, the supplied irradiation time and power (for these large portions of leaf and water) was not sufficient to produce phenolic content, and hence the yield dropped significantly.

Fig. 5b shows the impact of irradiation power on the oil yield. When the irradiation power increased to 640 W, the oil content increased, and then reduced when with a further increase in the power. This is because of the thermal degradation of the 1,8-cineole content due to strong exposure to microwave radiation. Thus, the maximum 1,8-cineole yield was achieved at 640 W and the value was 93.0%. A gradual decreasing trend was observed in the 1,8-cineole yield when the extraction power increased from 3 to 6 min (Fig. 5c). The maximum yield of 94.2% was observed at 4 min. When the exposure time increased at a moderate power of 480 W, overheating of the oil content led to the value-added products being denatured. The grinding of *Eucalyptus* leaves released the essential oil onto the surface of the plant particles, facilitating quicker extraction using water vapor.[59] Therefore, most of the oil was extracted within a very short time. Thus, 4 min of extraction time was confirmed to be experimentally sufficient.

3.4.2. Response surfaces for dependent variables. The RSM is a design tool to enhance the extraction process of plant functional components by optimizing the process parameters. The interaction relationship between the independent and dependent parameters was evaluated under the optimized conditions. In this study, the matrix was designed with 3 factors and 3 levels containing 13 experiments and presented in Table 2. In the ME, the extraction yield was influenced by different process parameters, which were pre-optimized earlier (Section 3.4.1). To increase the yield of 1,8-cineole, further optimization was investigated using RSM design. The experimental runs were carried out by varying the irradiation power levels (160–800 W), extraction time (1–10 min), and SSR (2–10 g mL^{-1}) to maximize the extraction yield of 1,8-cineole. The interaction effect of any two-process parameter significantly evaluates the impact of 1,8-cineole extraction from *Eucalyptus*.

The response surface plots for the combinations of several parameters, including SSR and extraction time, SSR and extraction power, and extraction time and irradiation power, are displayed in Fig. 5d–f. Initially, the extraction yields increased, and then progressively dropped when the SSR increased from 2

Table 3 Values of estimated model parameters for solid–liquid extraction of 1,8-cineole from *E. cinerea* in ultrasound-assisted extraction

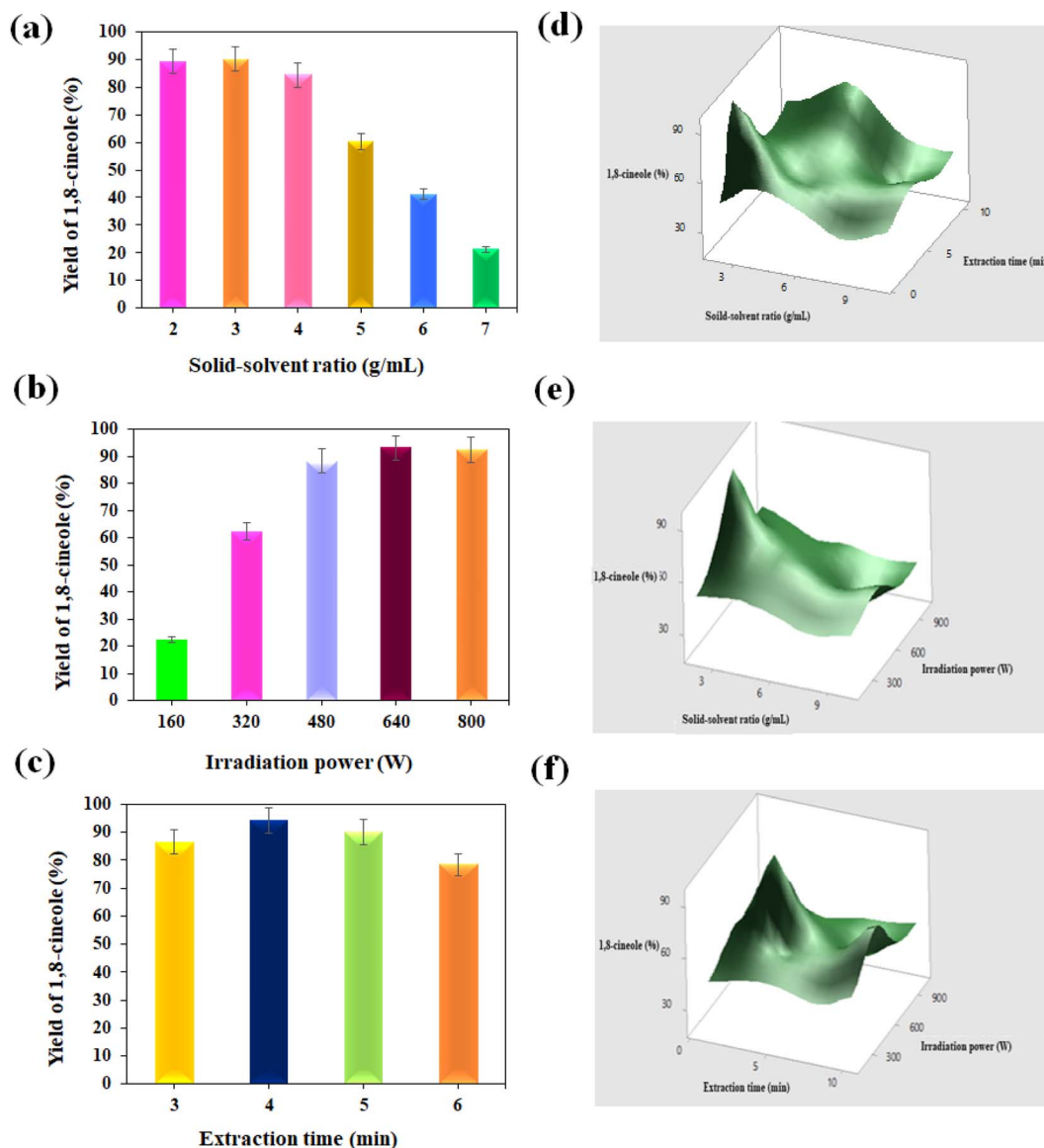| T/°C	Pseudo-first-order kinetics			Peleg model			Power law model		
	k_1 (min^{-1})	Y_1 (%)	R^2	K_1 (min^{-1})	K_2	R^2	K (min^{-1})	n	R^2
60	0.0183	69.571	0.984	0.053	1.775	0.998	2.398	0.4	0.979
27	0.0334	87.8835	0.981	1.186	0.819	0.997	0.908	0.5	0.989

Fig. 5 Graphical representation of the (a) effect of the solid–solvent ratio on the yield of 1,8-cineole in ME, (b) effect of irradiation power on the yield of 1,8-cineole in ME, (c) effect of extraction time on the yield of 1,8-cineole in ME, (d) interaction response effects of solid–solvent ratio and extraction time, (e) interaction response effects of irradiation power and the solid–solvent ratio, and (f) interaction response effects of irradiation power and extraction time.

to 10 g mL^{-1}, while the extraction power was fixed at a specific value. When the extraction time increased from 3 to 10 min, the yield first increased, and subsequently dropped (Fig. 5d). Thus, the extraction rate of eucalyptol utilizing the microwave approach was negatively impacted by both independent factors, *i.e.*, SSR and extraction time. Because the mass transfer principle is more consistent with a lower SSR, a lower ratio results in a larger driving force and higher diffusion.[60] Further, Fig. 5e confirms that the extraction time and irradiation power have a negative impact on the extraction of oil yield under a constant supply of SSR. This response surface demonstrated a significant interaction effect between all independent variables.

Fig. 5f represents the interaction surfaces between the extraction time and irradiation power when increasing the

extraction power at a constant feed of SSR, where the extraction yield increased and stabilized at 640 W. Simultaneously, very little extraction time is sufficient to extract the oil yield. Increasing the extraction time and irradiation power caused local burns in the raw materials.[61] Hence, a low extraction time (3 min) and high extraction power (640 W) are beneficial to improve the oil extraction under microwave-assisted conditions. The applied temperature (45 °C) and microwave power (640 W) significantly influence the microwave extraction time; consequently, the highest extraction was achieved at the shortest extraction time. We deduced that the largest amount of 1,8-cineole (95.62%) was achieved during a very short exposure time of around 4.5 min at a power of 640 W, with a minimum SSR of 2 g mL^{-1}. The extraction was conducted experimentally

under the identified optimum conditions in three repeated trials to validate the optimum conditions of the model. Finally, the average maximum 1,8-cineole yield of 95.48% was achieved through lab experiments, which is the near-optimal value of the model (95.62%). Thus, the designed model significantly determined the maximum essential oil yield from *E. cinerea*. In addition, this optimal condition is much more suitable to enhance the oil yield from plant sources under microwave conditions. Similar studies were conducted, and the results are consistent with the reports on extracting bioactive compounds from different plant sources.[24,58,62]

3.5. Chemical composition analysis of *Eucalyptus* essential oil extracted by different techniques

The extraction method, among other process parameters, significantly impacts the chemical composition of the essential oil produced from aromatic plants, which may affect its antibacterial and antioxidant qualities. Using the GC technique, the extracted free volatile oil profile from various extraction procedures was examined and verified.

Fig. S2a–d (ESI)† show the gas chromatograms employed for the analysis of extracted essential oil *via* the HD method for different runs. The available value-added compounds in the essential oil were analyzed for each run. Fig. S2a–d (ESI)† show the essential oil composition gas chromatograms for the different samples including big foliage (1 : 25 g mL^{-1}), small foliage (1 : 25 g mL^{-1}), big foliage (1 : 10 g mL^{-1}) and small foliage (1 : 10 g mL^{-1}), respectively, where the peaks observed at

~8.08 retention time belong to 1,8-cineole. The yield % of 1,8-cineole was identified for the samples of runs 1, 2, 3, and 4 to be 6.435%, 21.208%, 36.033%, and 72.151%, respectively. Among the four runs, the maximum oil yielded (run 4 : 3.5 mL) sample contains the highest concentration (72.151%) of 1,8-cineole in oil. Furthermore, it was observed that a maximum of 16 components was detected, and 1,8-cineole was deduced to be the principal substance in the highest percentage during HD extraction. Fig. 6a shows the gas chromatogram of the essential oil sample yielding the maximum 1,8-cineole from SE. The peak belonging to 1,8-cineole was observed at the retention time of ~8.685. The yield % of 1,8-cineole was identified as 69.01% and the profile showed nearly 32 components. Fig. 6b–d show the gas chromatogram of the results of the impact of sonication power, pH, and SSR on 1,8-cineole yield during ultrasound extraction. The 1,8-cineole peak was observed at a retention time of ~8.690. The yield % of 1,8-cineole was identified to be 49.56%, 59.02%, and 51.35% for the optimized ultrasonication power, pH, and SSR experiments, respectively. The enhanced 1,8-cineole yield observed using RSM was 74.48% under the optimized condition of SSR of 1 : 10 w/v, ethanol–water ratio of 20%, pH of 6, and sonication time of 70 min. The 1,8-cineole peak was observed at the retention time of ~8.688 and 1,8-cineole was found to be the maximum obtained compound (Fig. 7a).

Furthermore, the gas chromatograms of the ultrasonic-assisted kinetic extraction study-maximum oil yield samples (60 °C, 45 °C, and 27 °C) were also analyzed. Fig. 7b shows the
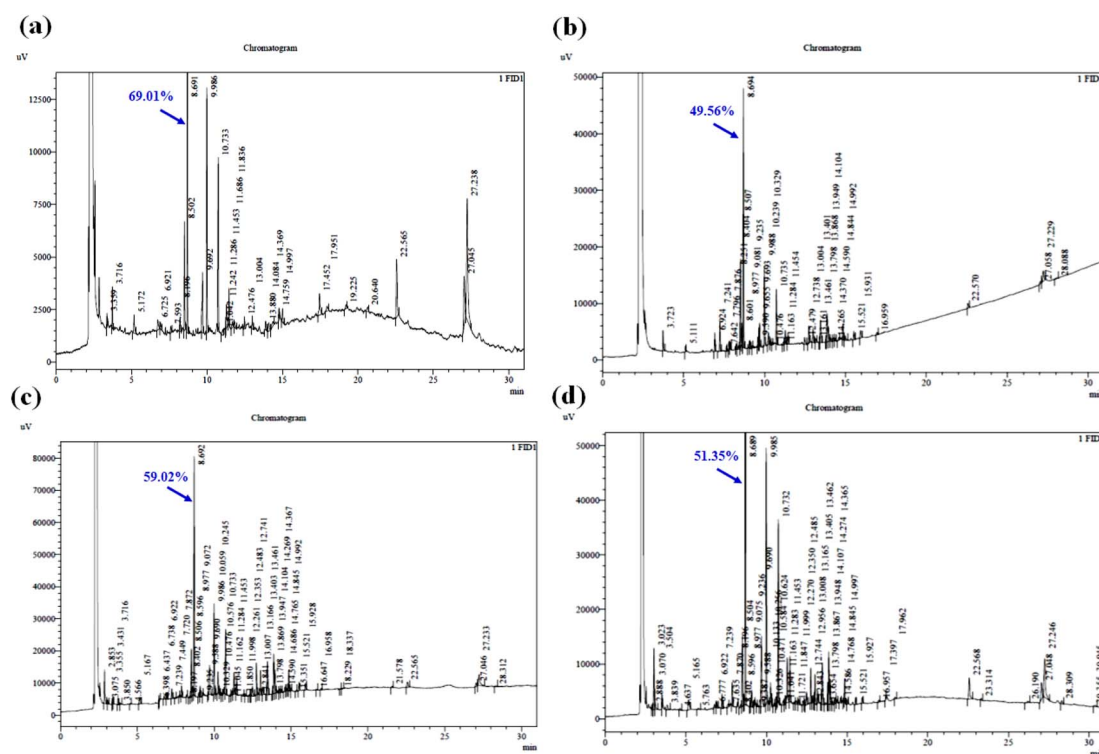

Fig. 6 Gas chromatogram of the essential oil composition studied for the (a) maximum yielded (69.01%) sample during SE, (b) maximum yielded sample (49.56%) at optimized sonication power (240 W) during UE, (c) maximum yielded sample (59.02%) at optimized pH (6) during UE and (d) maximum yielded sample (51.35%) at the optimized SSR ratio (1 : 10 w/v) during UE.
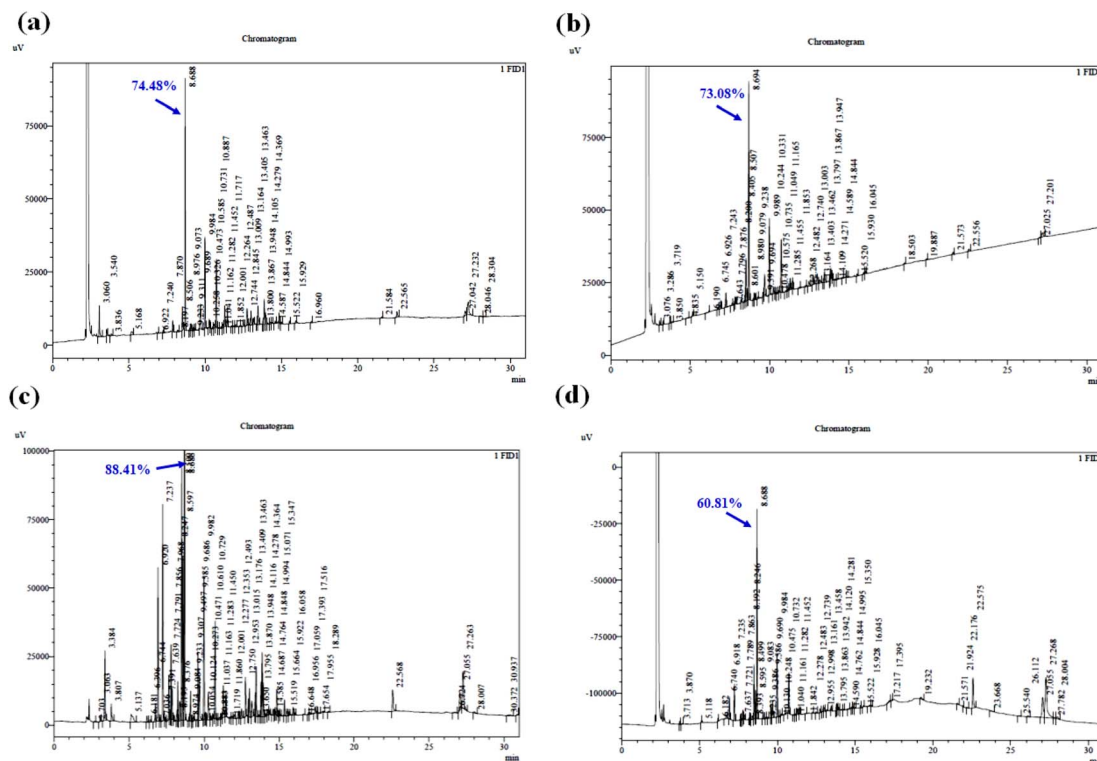
Fig. 7 Gas chromatogram of the essential oil composition studied for (a) maximum yielded (74.48%) sample under RSM optimal conditions for the UE process, (b) maximum yielded (73.08%) sample at 60 °C during UE kinetics, (c) maximum yielded (88.41%) sample at 45 °C during UE kinetics and (d) maximum yielded (60.81%) sample at 27 °C during UE kinetics.

gas chromatogram of the maximum yielded (73.08%) essential oil at 60 °C and the observed peak (~8.694) belongs to the retention time of the targeted compound. Fig. 7c illustrates the gas chromatogram of the maximum yielded (88.41%) essential oil at 45 °C and the observed peak (~8.686) corresponds to the retention time of 1,8-cineole. Fig. 7d shows the gas chromatogram of the maximum yielded (60.81%) essential oil at 27 °C and the observed peak (~8.688) corresponds to the retention time of 1,8-cineole. During, UE, 66 components were identified in the essential oil profile. Fig. 8a–c show the gas chromatogram of the ME results of the impact of irradiation power, solid–solvent ratio, and extraction time on 1,8-cineole yield during the microwave technique. The 1,8-cineole peak was observed at the retention time of ~3.890. The % yield of 1,8-cineole was identified to be 93.0%, 90.15%, and 94.2% for the optimized irradiation power, SSR, and extraction time experiments, respectively. The enhanced 1,8-cineole yield observed using RSM was 95.62% under the optimized condition of SSR of 2 g mL^{-1}, irradiation power of 640 W, and extraction time of 4.5 min. The 1,8-cineole peak was observed at the retention time of ~3.850, which was found to be the maximum compound obtained (Fig. 8d). During ME, the essential oil profile had nearly 31 components. The components found in the eucalyptus oils produced using the four processes were typically sesquiterpenes, oxygenated monoterpenes, and oxygenated sesquiterpenes. The most prevalent chemical in each sample was always 1,8-cineole, the primary oxygenated monoterpene advantageous essential oil component. The proposed oil

components in the essential oil varied based on the type of extraction method.

The concentration of oxygenated monoterpenes was found to be much lower in the extracted oil samples such as α-pinene, limonene, verbenone, cuminal, *p*-cymene, terpineol-4-ol, L-pinocarveol, thymol and L-perillaldehyde. The oxygenated sesquiterpenes are globulol, caryophyllene oxide, palustrol, cubenol, cadinol, ledol, *etc.* identified at different retention times. The other components were found to be >1% concerning the extraction methods. The observed results showed similar trends with the reported essential oil extracted from *E. cinerea* leaves using HD,[31] *E. camaldulensis* using HD,[17] *E. camaldulensis* using ME,[34] and *E. globulus* using UE.[33] However, due to the agro-climatic conditions of the *Eucalyptus* plant, the geological location, physical and age factor of the foliage, nature of the soil, extraction process, and period of test sample collection, the composition and chemical profile change compared to the results that are now accessible.[63] In addition, the oil sample chemical component and composition profile varied based on the chemotype/genotype of the plant source.[64] We inferred that the extracted essential oil from the ME method has better quality, which has plentiful bioactive components and economically viable value (1,8-cineole).

3.6. Impact of the morphology of *Eucalyptus* foliage during different extractions

SEM images assisted in understanding the extraction efficiency by visualizing the microstructural changes in the samples. The
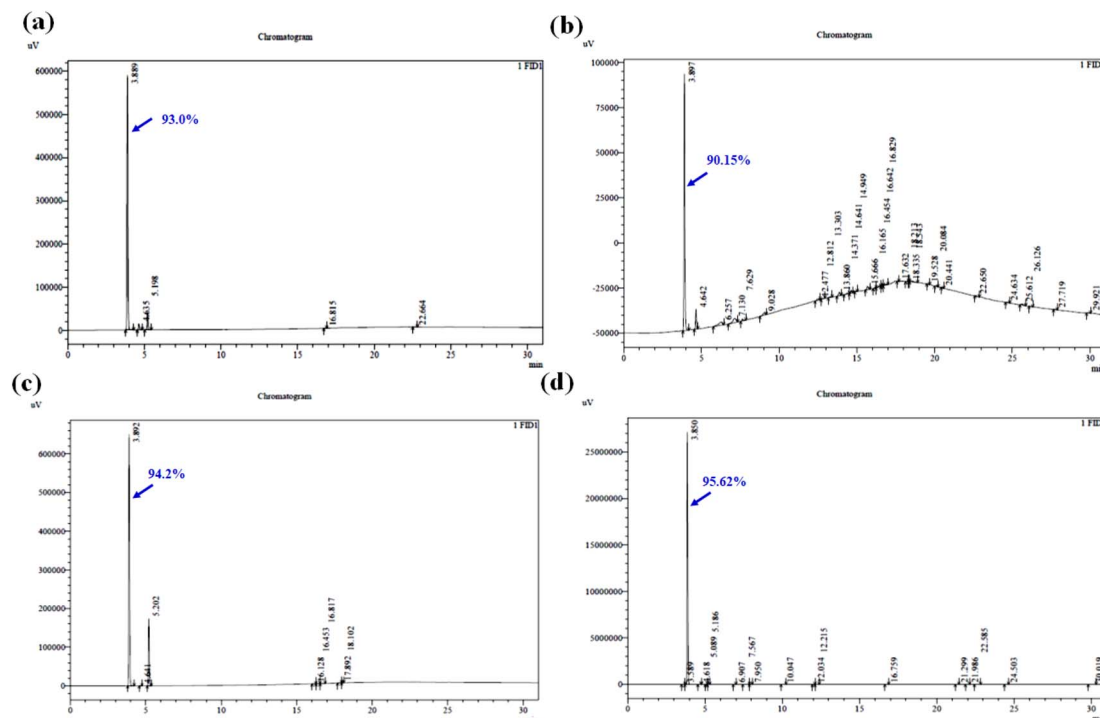
Fig. 8 Gas chromatogram of the essential oil composition studied for the (a) maximum yielded sample (93.0%) at the optimized irradiation power (640 W) during ME, (b) maximum yielded sample (90.15%) at the optimized SSR ratio (1 : 10 w/v) during ME, (c) maximum yielded sample (94.2%) at optimized extraction time, and (d) maximum yielded (95.62%) sample under RSM optimal condition for the ME process.

leaves of *E. cinerea* are oval/rounded in shape, dark green, densely reticulated, and have an abundance of oil glands. The tubular waxes on this plant conceal its oil glands, reducing their visibility.[65] The morphology characteristics of the *E. cinerea* leaf were analyzed using an SEM analyzer. Fig. 9a and b show the SEM micrographs of the adaxial and abaxial epidermal surface of the *E. cinerea* leaf before the extraction process, respectively. The main difference between the abaxial and adaxial stomata is usually the stomatal density is higher, while less stomatal density is on the adaxial surface of the leaf. It can be observed from Fig. 9a and b that the oil gland density was greater on the abaxial surface, whereas less on the adaxial surface. Additionally, as seen in Fig. 9c, the oil gland chambers appeared to be spherical to ellipsoidal. The two most noticeable structures were oil-filled tubes and plates with varying orientations. The entire leaf and its cuticle surfaces were heavily covered in glands. In addition, wax tubes with oil were principally found around both stomata.

Alternatively, the inner side cuticles of the leaf before and after extraction were also studied. Fig. 9d and e illustrate the SEM micrographs of the inner side cuticles of the leaf before and after extraction, respectively. Commonly, a rough topography and epidermal structures with granular patterns are presented in the intact cuticles. It seems that the isolated cuticle topography of the foliage residue became smoother (Fig. 9e) compared to the intact tissues before oil extraction (Fig. 9d). A noticeable structural change was observed in the image of the post-oil extraction residues. A plane dumpy cuticle and obvious papillae were identified and there were disrupted tissues in the

areas where oil has been extracted. The whole impression of the cuticle became visible and increased during extraction, and it seemed to be more fragile, indicating the occurrence of oil subjected to the extraction process. It was observed that SEM images are useful in observing the vascular bundle integrity, cell wall integrity, stomatal density and morphology, cuticle thickness and structure, and epidermal cell shape and size.

The SEM micrographs of the *E. cinerea* leaf residues after the different extraction processes are presented in the upcoming figures. Fig. 9f and 10a show the SEM image of the HD extraction foliage. The morphology of the spent leaf producing the maximum oil yield during optimization of the leaf size with SSR (72.151%) and kinetic studies (72.85%) is shown in Fig. 9f and 10a, respectively. Fig. 10b and c show the SEM image of the leaves treated by SE. The morphology of the spent leaf producing the maximum 1,8-cineole yield during optimization of SSR (68.07%) and optimization of extraction time (69.07%) is shown in Fig. 10b and c, respectively. Fig. 10d and e show the SEM images of the leaves treated by UE. Fig. 10d and e show the micrographs of the spent leaf obtained from the kinetic studies conducted at 45 °C and RSM optimization study and has the maximum extracted 1,8-cineole of 88.41% and 74.48%, respectively. Fig. 10f shows the image of the spent leaf obtained from the ME RSM optimization study where 95.62% of 1,8-cineole was extracted.

There are noticeable differences in the images in Fig. 9c and 10f, where the secretory structures are empty, the mesophyll cells are loosely packed or spongy, and the granular walls are ruptured. During hydro-distillation, the glandular trichomes
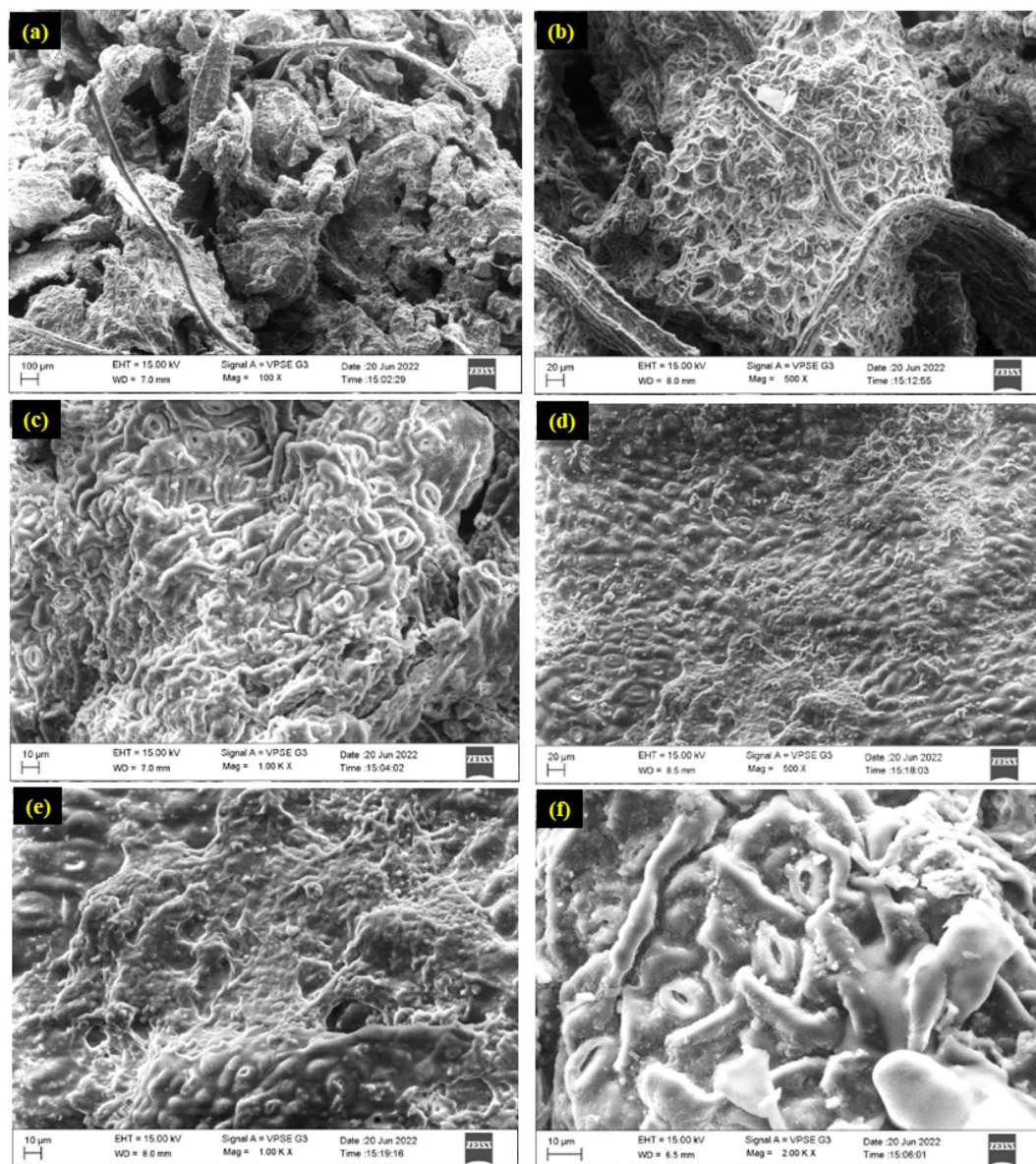
Fig. 9 SEM micrographs of (a) adaxial leaf surface of *E. cinerea* and (b) abaxial leaf surface of *E. cinerea*. (c) Overlying cells covering the secretory cavities in (d) inner side cuticles of the leaf before extraction, (e) inner side cuticles of the leaf after extraction and (f) spent leaves obtained after HD extraction (72.151%).

containing essential oils seem vacant (as large pores) but still intact due to the mild operating conditions. Similarly, the leaf residue has a substantial change in leaf structure, leading to a smoother surface layer, which confirms that the interaction between the leaf and ethanol during SE extended for a longer extraction time such as 6 h (Fig. 10b) and 9 h (Fig. 10c). During SE, the vascular bundles retained their form although at least 68.07% of the oil gland walls deteriorated to allow oil discharge.[66] During UE, a large portion of the porous structure appears to have collapsed due to the formation of cavity bubbles. In addition, the sonication power (240 W), elevated temperature, and extraction time (>50 min) contribute to huge destruction and large perforation on the plant epimerises, which ensures the effective release of 1,8-cineole from the *Eucalyptus* leaf.

Fig. 10e shows that the granular morphologies of the oil glands no longer had a high degree of deformation and the vascular bundles retained their structure throughout UE. During ME, huge deformation was observed in the plant epidermis initially due to the higher dielectric constant of water allowing more absorption of microwave energy within 4.5 min.[67] The absorbed irradiation (640 W) increased the localized temperature following the expansion of the oil glands, which contributed to the fast and easy rupture of the glandular walls. Hence, the maximum yield of 1,8-cineole was achieved under this condition, as confirmed by the image in Fig. 10f. According to the above-mentioned observations, the spent leaf no longer had a clear texture, showing distorted oil glands, and still appreciable bundles of vascular due to the different extraction methods, which led to the destruction of the oil components
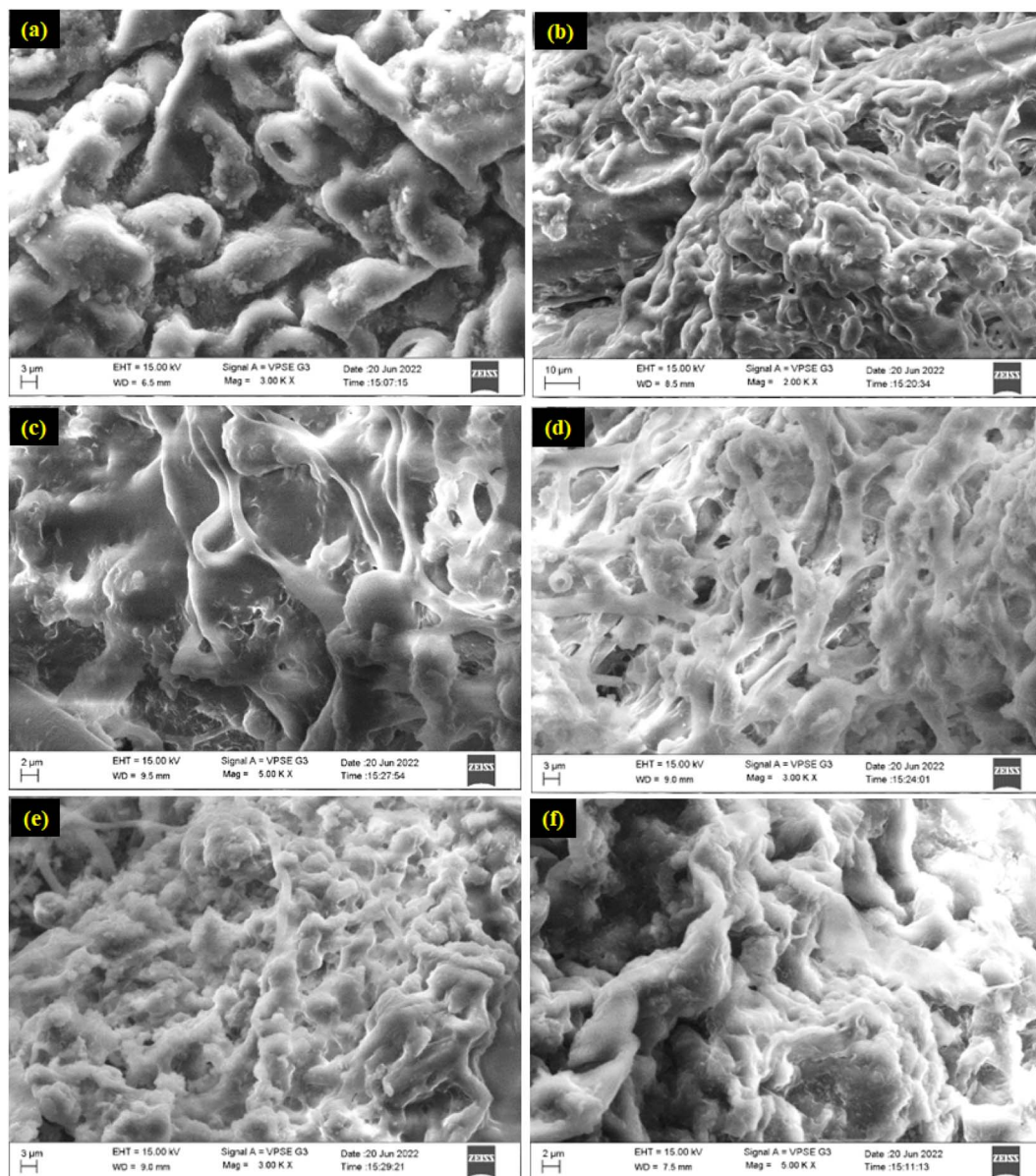
Fig. 10 SEM micrographs of the (a) spent leaf obtained after HD extraction during kinetic study (72.85%), (b) spent leaf obtained after SE during optimization of SSR (1 : 10 w/v), (c) spent leaf obtained after SE during optimization of extraction time (9 h), (d) spent leaf obtained from UE kinetic studies conducted at 45 °C, (e) spent leaf obtained during RSM optimization for UE and (f) spent leaf obtained during RSM optimization for ME.

and significant structure transformations in the plant material.[68] The SEM images helped to visualize the microstructural changes in the leaf texture, vascular bundles, and cell structure after extraction, revealing that the extraction progressed. Thus, observing the changes in the leaf microstructure assists in the optimization of the extraction process, which can help understand the extraction efficiency.

3.7. Comparison of different extraction methods to yield 1,8-cineole

Table 4 presents an overview of the extracted essential oil yield achieved by different extraction methods, including HD, SE, UE, and ME. The impact of the different extraction methods on the

yield of 1,8-cineole was significant. Comparing the oil yield of the two conventional extraction methods, HD (72.85%) method achieved a higher yield of 1,8-cineole than SE (68.07%). Nearly, 32 chemical components were identified in SE and 16 chemical components were identified in HD. Although the essential oil quality was monitored at SE, the HD approach is more economically viable due to its high concentration of 1,8-cineole extracted. In this investigation, HD produced a lower yield, while SE with ethanol produced the maximum yield, and similar results were reported elsewhere.[41,44] Compared to the conventional extraction method, the contemporary technologies yielded a higher quantity of essential oil.[24,69] Compared to modern strategies, a maximum yield of targeted components was observed in ME (95.62%) than UE (74.48%). Indeed, 66

Table 4 Comparison of different optimum process parameters for various extraction methods

Parameters	Hydro-distillation	Soxhlet extraction	Ultrasonic-assisted extraction	Microwave-assisted extraction
Extraction time (min)	180	360	70	4.5
Solid to solvent ratio (g mL^{-1})	1:10	1:10	1:10	2
pH	7	7	6	7
Power (W)	—	—	240	640
Temperature (°C)	100	100	45	60
1,8-Cineole (%)	72.85	68.07	74.48	95.62

chemical components were identified from UE-extracted oil, whereas 31 were identified in the microwave extraction. Compared with other extraction parameters of these methods, microwave extraction yielded the components within a short period (4.5 min) compared to the 70 min in the UE method. This is due to its advantages of irradiation power (640 W), less water consumption, less irradiation time, faster polarization, and huge decomposition of oil glands in the foliage.

Modern technologies have the potential to extract better-quality oil from biomass sources.[70,71] Table 5 shows a comparison of the extracted 1,8-cineole yield in the essential oil derived from different *Eucalyptus* species. According to the observation, the present study satisfied the research gap on the composition of essential oil extracted from *E. cinerea* leaves. This is the first and good reference reporting experiments with SE, UE, and solvent-free ME to extract 1,8-cineole from *E. cinerea* species. Gullón *et al.*[50] evaluated the specific energy consumption during HD, ME, and UE, and the values were found to be 0.177, 0.013, and 0.082 kW h per g GAE, respectively, for oil extraction from *E. globulus*. ME yielded the lowest specific energy usage, which was more than 13 times lower than other conventional extraction methods. Therefore, the ME method was more effective and yielded the maximum 1,8-cineole from *E. cinerea* leaves. Furthermore, this process can be a viable environmentally friendly substitute for traditional extraction techniques.

3.8. Mechanism adopted during the different extraction processes

Different types of interaction mechanisms have been reported for different extraction processes. The interactions between the solvent component and target compound (1,8-cineole) are related to the process variables including extraction time, solvent consumption, temperature, type of solvent, SSR, and irradiation power. The intermolecular interaction is subjected to hydrogen bond interaction between the solvent molecule and 1,8-cineole. Additionally, given that most of the negative charge of 1,8-cineole is concentrated around oxygen atoms, additional atoms can readily enclose it in a cavity.[82] A hydrogen bond contact is created between the oxygen atom of 1,8-cineole and the hydrogen atom of the hydroxyl group in the solvent (ethanol/water). Furthermore, the polar solvent of ethanol effectively attracts many polar compounds containing O–H bonds such as 1,8-cineole and other bio-active compounds.

One feasible justification for the observed variations in the chemical components is that each component has a distinct

extraction process. Given that water solvent does not immediately dissolve the organic compounds in hydro-distillation, the plant sample was submerged in water and heated to 100 °C. Thus, the components in the oil glands desorb from the leaf surface, and then diffuse into the aqueous phase, where the azeotropic mixture is formed, and gradually evaporated and condensed. In this process, the free volatile oil compounds are easily extracted than heavier compounds with higher boiling points.[41] In contrast, ethanol solvent was used in SE in this study. Due to the polar nature of ethanol, it can extract more polar organic compounds and non-polar components compared to hexane solvent. The oil component and solvent interaction is different from that in the SE and HD methods. There are four main processes involved in the SE process, as follows: (1) solvent diffusion, (2) extracted substance dissolution, (3) internal diffusion of the substrate and solvent, and (4) external diffusion of the substrate and solvent. The solvent is first heated to reflux before dripping into the thimble and diffusing into the matrix of vegetation. Following that, the solvent and bio-active compound mixture diffuses back into the bulk aqueous phase from the surface of the foliage. Once the solution level reaches the top of the siphon arm, it backflows into the lower flask. Besides, ethanol Soxhlet extracts waxes and chlorophyll (heavy components), which were not detected by GC analysis.[83]

High-frequency sound waves or ultrasound waves travel at frequencies greater than 20 kHz and are produced in liquids *via* rarefaction and compression. Cavitation is the collapse of vapor bubbles caused by pressure greater than the tensile strength of a liquid. The implosion of the cavitation bubbles, which causes high velocity interparticle collision and disruption in the microporous particles of the leaves, is thought to be the source of macroturbulence.[84] The microjets cause foliage surface peeling, erosion, component breakdown, and release of bioactive components from the leaf matrix through impingement. This is owing to the mass transfer mechanism of eddy and internal diffusion. Therefore, it can be stated that the two important elements improving the extraction with ultrasonic power are cell rupture and efficient mass transfer. Several reports have confirmed that the essential oil composition was not desaturated using ultrasonic wave propagation.[85,86]

The ME method transfers microwave energy (300 MHz to 300 GHz) to the heated solvent of ethanol–water solution for polar organic compounds *via* two mechanisms, *i.e.*, dipole rotation and ionic conduction.[87] Because of the impact of microwaves,

Table 5 Comparison of extracted 1,8-cineole yield in the essential oil derived from different *Eucalyptus* species

Eucalyptus species	Extraction method	Operating conditions	1,8-Cineole yield	Reference
Eucalyptus globulus	Ultrasound extraction	Sample: 10 g; pH: 5, temperature: 50 °C, % ethanol in water: 15, ultrasound power: 40 W and ultrasound time: 15 min	67.29%	Palma et al.[33]
Eucalyptus globulus	Steam distillation by ultrasound pre-treatment	Sample: 100 g; ultrasound power: 70 W, ultrasound time: 10 min; reactor size: 3 L; temperature: 100 °C	2.22 mL/100 g at 260 min	Mei et al.[72]
	Water distillation by ultrasound pre-treatment		2.21 mL/100 g at 290 min	
Eucalyptus globulus	Soxhlet extraction	Sample: 10 g; extraction time: 4 h; solvent ratio: 1 : 10 w/v; solvents: methanol, chloroform and hexane	48.2% for methanol, 35.5% for chloroform and 5.8% for hexane	Nile and Keum[73]
Eucalyptus globulus	Hydro-distillation	—	63.8%	Luís et al.[74]
Eucalyptus saligna	Hydro-distillation	Sample: 500 g; time: 4 h; solvent: water	24.26%	Bett et al.[75]
Eucalyptus camaldulensis, Eucalyptus crebra, Eucalyptus tereticornis, Eucalyptus globules, Eucalyptus melanophloia, Eucalyptus microtheca	Hydro-distillation	Sample: 50 g; solvent: water	16.1%, 4.9%, 15.2%, 56.5%, 3.1% and 2.0%, respectively	Ghaffar et al.[76]
Eucalyptus cinerea	Hydro-distillation	Time: 2 h; solvent: water	88.5%	Rossi and Palacios[77]
Eucalyptus maiden, Eucalyptus astringens, Eucalyptus cinerea, Eucalyptus leucoxylon, Eucalyptus lehmannii, Eucalyptus sideroxylon, Eucalyptus bicostata	Water distillation	Sample: 100 g, time: 3 h	83.59%, 60.01%, 79.18%, 77.76%, 49.07%, 80.75%, and 81.29%, respectively	Sebei et al.[78]
Eucalyptus camaldulensis	Hydro-distillation	Sample: 5 g; time: 3 h	31.43%	Abbas et al.[63]
	Supercritical fluid extraction	Sample: 5 g; time: 60 min; temperature: 45 °C; CO$_2$ flow rate: 10 mL min^{-1}	31.10%	
Eucalyptus urophylla	Steam distillation	Sample: 200 g; humidity: 70–90%; temperature: 96.5 °C, pressure: 0.92 atm; time: 4 h	18.2–45.5%	Achmad et al.[79]
Eucalyptus globulus	Microwave-assisted extraction	Solid–water ratio: 1 : 3 mL g; time: 60 min, irradiation power: 450 W	38.771%	Tran et al.[80]
Eucalyptus globulus	Solid-phase microextraction	Sample: 2 g; fibre: PDMS 10 μm thickness; temperature: 60 °C; time: 20 min; sonication time 10 min	51.25%	Abbasi et al.[81]
Eucalyptus cinerea	Hydro-distillation	Sample: 1 kg; time: 3 h	85.1%	Mann et al.[30]
	Supercritical fluid extraction	Sample: 1.5 kg; time: 1 h; temperature: 60 °C; CO$_2$ flow rate: 60 g min; pressure: 140 bar	70.4%	
Eucalyptus cinerea and *Eucalyptus camaldulensis*	Hydro-distillation	Sample: 100 g; time: 3 h	64.89% and 45.71%	Herzi et al.[31]
	Supercritical fluid extraction	Sample: 50 g; time: 30 min; temperature: 40 °C; CO$_2$ flow rate: 20 g min; pressure: 90 bar	16.10% and 1.74%	
Eucalyptus oleosa	Hydro-distillation	Sample: 50 g; time: 90 min	15.31%	Romdhane et al.[67]
	Microwave-assisted extraction	Sample: 50 g; time: 25 min; irradiation power: 600 W	25.65%	
Eucalyptus camaldulensis	Steam distillation	Sample: 300 g	21.79%	Saleh et al.[17]
	Hydro-distillation	Sample: 300 g	17.74%	
	Superheated steam distillation	Sample: one kg; temperature: 150 °C	21.43%	
	Hydro-distillation	Sample: 15 g; time: 3 h	70.03%	

© 2024 The Author(s). Published by the Royal Society of Chemistry

Table 5 (Contd.)

Eucalyptus species	Extraction method	Operating conditions	1,8-Cineole yield	Reference
Eucalyptus loxophleba ssp. *lissophloia*	Soxhlet extraction	Sample: 5 g; time: 8 h; solvent: ethanol and hexane; temperature: 90 °C	29.85% for ethanol solvent	Zhao and Zhang[41]
	Supercritical fluid extraction	Sample: 5 g; time: 30 min; temperature: 20 °C; CO_2 flow rate: 2 L min; ethanol range: 5–15 vol%, pressure: 10 MPa	46.19%	
Eucalyptus urograndis	Microwave-assisted extraction	Sample: 200 g; solid–liquid ratio: 1 : 3 g mL; time: 40 min; irradiation power: 360 W; stirring speed: 400 rpm	39.30%	Lainez-Cerón et al.[56]
Eucalyptus cinerea	Hydro-distillation	Sample: 100 g; solid–solvent ratio: 1 : 10 g mL; solvent: water, time: 3 h; temperature: 100 °C, pH: 7	72.85%	Present study
	Soxhlet extraction	Sample: 100 g; solid–solvent ratio: 1 : 10 g mL; solvent: ethanol, time: 9 h; temperature: 100 °C, pH: 7	69.01%	
	Ultrasound-assisted extraction	Sample: 100 g; solid–solvent ratio: 1 : 10 g mL; ethanol–water ratio: 20 v%, time: 50 h; temperature: 45 °C, pH: 6; ultrasound power: 240 W	88.41%	
	Microwave-assisted extraction	Sample: 100 g; solid–solvent ratio: 2 g mL; time: 4.5 min; temperature: 60 °C, pH: 7, irradiation power: 640 W	95.62%	

the moisture content in the plant matrix may evaporate inside the cell, creating a high pressure, which causes the plant cell to swell. This causes the cell wall to be pushed, stretched, and eventually ruptured, releasing the bioactive substances. In practice, the high-temperature hydrolysis of cellulose bonds caused by microwave radiation occurs in 3–4 min, converting the bonds into soluble portions. Exudation of the chemical components present in the cell into the surrounding solvents occurs during the extraction process. In addition, permeation and solubilization contribute to the release of the oil compounds from the plant matrix. Due to the localized heating, the oil components in the granular matrix and vascular systems are easily extracted and induced to flow toward the organic solvent. This approach is well suitable for extracting essential oil components and preventing their degradation from microwave irradiation.[88,89]

4. Conclusion and outlook

To date, most investigations on the extraction of essential oils from *Eucalyptus* leaves have been focused on different species, with little interest paid to *Eucalyptus cinerea* using different extraction methods. Thus, the present study aimed to extract a high percentage yield of 1,8-cineole from *E. cinerea* leaves.

During hydro-distillation, a maximum yield of 1,8-cineole (72.85%) was obtained for small-size leaves (2 cm) under a minimum SSR ($1 : 10$ g mL^{-1}) within a short time (4 h). The experimental data fit first-order extraction kinetics with an R^2 value of 0.9988, leading to an extraction rate constant of $K = 0.0131$ min^{-1}. During SE, the yield of 1,8-cineole increased (68.07%) up to the SSR of $1 : 10$ g mL^{-1}, and the maximum 1,8-cineole yield was found to be 69.01% at 9 h under the evaluation of the effect of extraction time. UE was carried out using the predetermined optimum conditions of sonication power (240 W), pH (6), and SSR ($1 : 10$ w/v) and yielded 49.56%, 59.02%, and 51.35% of 1,8-cineole, respectively. The maximum oil yield of 74.48% was achieved using RSM design and the optimal condition of ethanol–water ratio of 20 vol%, pH of 6, and extraction time of 70 min. Further, the kinetic analysis was investigated at different temperatures of 27 °C, 45 °C, and 60 °C using three empirical models of pseudo-first-order kinetics, the Peleg model, and the power law model. At 45 °C, the concentration of eucalyptol increased when the extraction increased time up to 50 min and the oil yield of 88.41% was achieved during ultrasound extraction.

The single-factor pre-optimization of irradiation power, SSR, and extraction time was performed for ME. Among the methods, RSM optimization of the microwave extraction resulted in a higher yield of 1,8-cineole (95.62%) under the optimal conditions of SSR of 2 g mL^{-1}, extraction time of 4.5 min and irradiation power of 640 W. During chemical component analysis, 16, 32, 66 and 31 bioactive components were identified with 1,8-cineole in the extracted oil, which belongs to the oxygenated monoterpenes, sesquiterpenes and oxygenated sesquiterpenes. The morphology investigation of the *E. cinerea* leaf residues before and after the process was illustrated and it was identified that the spent leaf no longer had a clear texture, solidly destructed oil glands, and still appreciable vascular bundles after the extraction. The different types of interaction mechanisms were reported for each extraction method and it was found that the intermolecular interaction is subjected to hydrogen bond interaction between the solvent molecule and 1,8-cineole-like value-added component.

Although some outcomes showed fruitfulness, others require further investigation. Research on the novel medical functions of *E. cinerea* needs attention to exploit its commercial benefits. Moreover, essential oil has a strong toxicity effect on various kinds of microbes and insects, and hence further study is suggested. The process of extracting 1,8-cineole from *E. cinerea* leaves is still not fully industrialized although an excessive amount of associated biomass is wasted annually. Thus, complete resource utilization can be accomplished by using *E. cinerea* leaves and solvent-free ME to extract essential oils effectively. This method is beneficial with a significant reduction in water, time, and energy consumption and added-value of *E. cinerea* resources. However, more research is required to assess its activity and economic features under ideal circumstances and make it much more suitable for low-budget industries.

Data availability

The authors confirm that the data supporting the findings of this study are available within the article and ESI.†

Author contributions

Conceptualization: D. B., R. G.; methodology: D. B., R. G., H.-S. B.; formal analysis: D. B., M. S.; data curation: D. B., M. S.; investigation: R. G., H.-S. B.; visualization: D. B., R. G.; validation: D. B., H.-S. B.; writing original draft: D. B.; software: M. S.; supervision: R. G., H.-S. B.; writing – review and editing: D. B., H.-S. B.; funding acquisition: H.-S. B.; project administration: H.-S. B., R. G. All authors have approved the final version of the manuscript.

Conflicts of interest

There are no conflicts that need to be declared.

Acknowledgements

References

1 K. Grewal, J. Joshi, S. Rathee, S. Kaur, H. P. Singh and D. R. Batish, *J. Essent. Oil Bear. Plants*, 2022, **25**, 419–429.

2 D. P. de Sousa, R. O. S. Damasceno, R. Amorati, H. A. Elshabrawy, R. D. de Castro, D. P. Bezerra, V. R. V. Nunes, R. C. Gomes and T. C. Lima, *Biomolecules*, 2023, **13**, 1144.

3 C. C. Hoch, J. Petry, L. Griesbaum, T. Weiser, K. Werner, M. Ploch, A. Verschoor, G. Multhoff, A. B. Dezfouli and B. Wollenberg, *Biomed. Pharmacother.*, 2023, **167**, 115467.

4 J. F. Campos and S. Berteina-Raboin, *Catalysts*, 2022, **12**, 48.

5 A. K. Dhakad, V. V. Pandey, S. Beg, J. M. Rawat and A. Singh, *J. Sci. Food Agric.*, 2018, **98**, 833–848.

6 Z. M. Cai, J. Q. Peng, Y. Chen, L. Tao, Y. Y. Zhang, L. Y. Fu, Q.-D. Long and X. C. Shen, *J. Asian Nat. Prod. Res.*, 2021, **23**, 938–954.

7 L. Dao, Y. Dong, L. Song and C. Sa, *Curr. Drug Delivery*, 2024, **21**, 697–708.

8 I. Amri, M. Khammassi, R. Ben Ayed, S. Khedhri, M. B. Mansour, O. Kochti, Y. Pieracci, G. Flamini, Y. Mabrouk, S. Gargouri, M. Hanana and L. Hamrouni, *Plants*, 2023, **12**, 816.

9 C. Danna, P. Malaspina, L. Cornara, A. Smeriglio, D. Trombetta, V. De Feo and S. Vanin, *Crop Prot.*, 2024, **176**, 106319.

10 L. C. A. Barbosa, C. A. Filomeno and R. R. Teixeira, *Molecules*, 2016, **21**, 1671.

11 A. K. Surbhi, S. Singh, P. Kumari and P. Rasane, *Adv. Tradit. Med.*, 2023, **23**, 369–380.

12 S. Mariappan and R. Issac, *J. Curr. Sci. Technol.*, 2022, **12**, 372–390.

13 I. Akhtar, S. Javad, T. Iftikhar, A. Tariq, H. Majeed, A. Ahmad, M. Arfan and M. Zia-Ul-Haq, in *The COVID-19 Pandemic*, Apple Academic Press, Taylor & Francis, 2022, pp. 393–445.

14 G. D. K. Babu and B. Singh, *Biochem. Eng. J.*, 2009, **44**, 226–231.

15 I. Mediavilla, M. A. Blázquez, A. Ruiz and L. S. Esteban, *Molecules*, 2021, **26**, 2379.

16 R. Kant and A. Kumar, *Sustainable Chem. Pharm.*, 2022, **30**, 100829.

17 M. T. Saleh, M. A. Ayub, M. Shahid, M. H. Raza, A. Hussain and T. Javed, *Iran. J. Pharm. Sci.*, 2023, **19**, 139–155.

18 H. M. AL-Chaabawi and D. K. Satmbekova, *J. Surv. Fish Sci.*, 2023, **10**, 3329–3336.

19 T. Kariyawasam, G. S. Doran, J. A. Howitt and P. D. Prenzler, *Environ. Toxicol. Chem.*, 2023, **42**, 982–994.

20 A. R. Mankar, A. Pandey and K. Pant, *Bioresour. Technol.*, 2022, **345**, 126528.

21 A. Famakinwa, J. Ilo, O. Olubi, O. O. Oguntibeju, J. Van Wyk and A. Obilana, *Curr. Res. Nutr. Food Sci. J.*, 2023, **11**, 910–940.

22 B. Gullon, A. Muniz-Mouro, T. A. Lú-Chau, M. T. Moreira, J. M. Lema and G. Eibes, *Ind. Crops Prod.*, 2019, **138**, 111473.

23 M. Narayanan, D. Baskaran and V. Sampath, *Sep. Sci. Technol.*, 2022, **57**, 707–718.

24 R. Govindarasu, D. Baskaran, P. Vignesh and P. S. R. Nannapuraju, *Biomass Convers. Biorefin.*, 2024, **14**, 10585–10598.

25 N. Yoshikawa, in *RF Power Semiconductor Generator Application in Heating and Energy Utilization*, Springer, Singapore, 2020, pp. 71–89.

26 B. Yingngam, A. Brantner, M. Treichler, N. Brugger, A. Navabhatra and P. Nakonrat, *Ind. Crops Prod.*, 2021, **165**, 113443.

27 A. Filly, A. S. Fabiano-Tixier, C. Louis, X. Fernandez and F. Chemat, *C. R. Chim.*, 2016, **19**, 707–717.

28 D. Baskaran, K. Chinnappan, R. Manivasagan and D. K. Mahadevan, *Chem. Data Collect.*, 2018, **15**, 143–152.

29 T. Paul, D. Baskaran, K. Pakshirajan, G. Pugazhenthi and R. Rajamanickam, *Environ. Technol. Innovation*, 2021, **21**, 101326.

30 T. S. Mann, G. D. K. Babu, S. Guleria and B. Singh, *Nat. Prod. Commun.*, 2011, **6**, 107–110.

31 N. Herzi, J. Bouajila, S. Camy, S. Cazaux, M. Romdhane and J. S. Condoret, *J. Food Sci.*, 2013, **78**, C667–C672.

32 B. Tesfaye and T. Tefera, *Int. J. Adv. Eng. Manage. Sci.*, 2017, **3**, 239870.

33 A. Palma, M. J. Díaz, M. Ruiz-Montoya, E. Morales and I. Giráldez, *Ultrason. Sonochem.*, 2021, **76**, 105654.

34 S. Li, F. Chen, J. Jia, Z. Liu, H. Gu, L. Yang, F. Wang and F. Yang, *Sep. Purif. Technol.*, 2016, **168**, 8–18.

35 I. Psarrou, A. Oreopoulou, D. Tsimogiannis and V. Oreopoulou, *Molecules*, 2020, **25**, 4520.

36 A. A. Ayoola, V. C. Efeovbokhan, O. T. Bafuwa and O. T. David, *Int. J. Sci. Technol.*, 2014, **4**, 66–70.

37 V. P. Katekar, A. B. Rao and V. R. Sardeshpande, *Sustainable Chem. Pharm.*, 2022, **29**, 100783.

38 H. S. Kusuma and M. Mahfud, *J. Appl. Res. Med. Aromat. Plants*, 2017, **100**, 46–54.

39 N. Z. Immaroh, D. E. Kuliahsari and S. D. Nugraheni, *IOP Conf. Ser.: Mater. Sci. Eng.*, 2021, **733**, 012103.

40 T. P. Dao, N. Q. Tran and T. T. Tran, *Mater. Today*, 2022, **51**, 172–177.

41 S. Zhao and D. Zhang, *Sep. Purif. Technol.*, 2014, **133**, 443–451.

42 M. Samadi, Z. Z. Abidin, R. Yunus, D. R. A. Biak, H. Yoshida and E. H. Lok, *Chin. J. Chem. Eng.*, 2017, **25**, 216–222.

43 J. Ye, S. Zheng, Z. Zhang, F. Yang, K. Ma, Y. Feng, J. Zheng, D. Mao and X. Yang, *Bioresour. Technol.*, 2019, **274**, 518–524.

44 O. R. Alara, N. H. Abdurahman and C. I. Ukaegbu, *J. Appl. Res. Med. Aromat. Plants*, 2018, **11**, 12–17.

45 V. H. Rodrigues, M. M. de Melo, I. Portugal and C. M. Silva, *J. Supercrit. Fluids*, 2018, **135**, 263–274.

46 J. C. Martínez-Patiño, B. Gullón, I. Romero, E. Ruiz, M. Brnčić, J. S. Žlabur and E. Castro, *Ultrason. Sonochem.*, 2019, **51**, 487–495.

47 T. G. Leighton, in *Ultrasound in Medicine*, CRC Press, Taylor & Francis, 2020, pp. 199–224.

48 A. M. Tamidi, K. K. Lau and S. H. Khalit, *Comput. Chem. Eng.*, 2021, **155**, 107498.

49 V. A. González-de-Peredo, M. Vázquez-Espinosa, E. Espada-Bellido, M. Ferreiro-González, C. Carrera, M. Palma and J. Ayuso, *Agronomy*, 2020, **10**, 966.

50 B. Gullón, P. Gullón, T. A. Lú-Chau, M. T. Moreira, J. M. Lema and G. Eibes, *Ind. Crops Prod.*, 2017, **108**, 649–659.

51 D. J. Bhuyan, Q. V. Vuong, A. C. Chalmers, I. A. van Altena, M. C. Bowyer and C. J. Scarlett, *S. Afr. J. Bot.*, 2017, **112**, 180–185.

52 S. Wang, A. H. M. Lin, Q. Han and Q. Xu, *Processes*, 2020, **8**, 1665.

53 I. A. A. Meziane, N. Bali, N. B. Belblidia, N. Abatzoglou and E. H. Benyoussef, *J. Appl. Res. Med. Aromat. Plants*, 2019, **15**, 100226.

54 A. Cvetković, T. Jurina, D. Valinger, A. N. A. Jurinjak Tušek, M. Benković and J. Gajdoš Kljusurić, *Croat. J. Food Sci. Technol.*, 2018, **10**, 64–72.

55 P. L. Kiew, M. D. Mashitah and Z. Ahmad, *J. Korean Soc. Appl. Biol. Chem.*, 2014, **57**, 53–66.

56 E. Lainez-Cerón, A. López-Malo, E. Palou and N. Ramírez-Corona, *Int. J. Food Eng.*, 2022, **18**, 129–142.

57 F. Al-Mamoori and R. Al-Janabi, *Int. Res. J. Pharm.*, 2018, **9**, 22–29.

58 C. Wei, C. Wan, F. Huang and T. Guo, *Oil Crop Sci.*, 2023, **8**, 7–15.

59 V. P. Pavićević, M. S. Marković, S. Z. Milojević, M. S. Ristić, D. S. Povrenović and V. B. Veljković, *J. Chem. Technol. Biotechnol.*, 2016, **91**, 883–891.

60 U. Yiğit, E. Turabi Yolaçaner, A. Hamzalıoğlu and V. Gökmen, *J. Food Process. Preserv.*, 2022, **46**, e16120.

61 H. Hannachi, H. Benmoussa, E. Saadaoui, I. Saanoun, N. Negri and W. Elfalleh, *J. Biotechnol.*, 2019, **14**, 7–17.

62 A. Dobrinčić, M. Repajić, I. E. Garofulić, L. Tuđen, V. Dragović-Uzelac and B. Levaj, *Processes*, 2020, **8**, 1008.

63 A. Abbas, F. Anwar, S. M. Alqahtani, N. Ahmad, S. H. Al-Mijalli, M. Shahid and M. Iqbal, *Dose-Response*, 2022, **20**, 1–12.

64 A. Ghasemi Pirbalouti, F. Malekpoor and A. Salimi, *Trends Phytochem. Res.*, 2017, **1**, 3–8.

65 P. Malaspina, M. Papaianni, M. Ranesi, F. Polito, C. Danna, P. Aicardi, L. Cornara, S. L. Woo and V. De Feo, *Plants*, 2022, **11**, 2777.

66 H. Boumediri, A. Bezazi, G. G. Del Pino, A. Haddad, F. Scarpa and A. Dufresne, *Carbohydr. Polym.*, 2019, **222**, 114997.

67 M. Romdhane, H. Bendaoud, E. Saadaoui and W. Elfalleh, *Arab. J. Med. Aromat. Plants*, 2019, **5**, 35–46.

68 A. K. Jha and N. Sit, *Trends Food Sci. Technol.*, 2022, **119**, 579–591.

69 C. Bitwell, S. S. Indra, C. Luke and M. K. Kakoma, *Sci. Afr.*, 2023, **19**, e01585.

70 *Essential Oils: Extraction Methods and Applications*, ed. I. Inamuddin, T. Altalhi and J. N. Cruz, Scrivener Publishing llc, John Wiley & Sons, United States, 2023.

71 M. M. A. N. Ranjha, S. M. Zahra, S. Irfan, B. Shafique, R. Noreen, U. F. Alahmad, S. Liaqat and S. Umar, in *Essential Oils*, Academic Press, Elsevier, United States, 2023, pp. 37–52.

72 X. Y. Mei, Y. Kitamura, K. Takizawa, A. Kikuchi and K. Watanabe, *Biomass Convers. Biorefin.*, 2014, **4**, 285–292.

73 S. H. Nile and Y. S. Keum, *Indian J. Exp. Biol.*, 2018, **56**, 734–742.

74 A. Luís, Â. Duarte, J. Gominho, F. Domingues and A. P. Duarte, *Ind. Crops Prod.*, 2016, **79**, 274–282.

75 P. K. Bett, A. L. Deng, J. O. Ogendo, S. T. Kariuki, M. Kamatenesi-Mugisha, J. M. Mihale and B. Torto, *Ind. Crops Prod.*, 2016, **82**, 51–62.

76 A. Ghaffar, M. Yameen, S. Kiran, S. Kamal, F. Jalal, B. Munir, S. Saleem, N. Rafiq, A. Ahmad, I. Saba and A. Jabbar, *Molecules*, 2015, **20**, 20487–20498.

77 Y. E. Rossi and S. M. Palacios, *Ind. Crops Prod.*, 2015, **63**, 133–137.

78 K. Sebei, F. Sakouhi, W. Herchi, M. L. Khouja and S. Boukhchina, *Biol. Res.*, 2015, **48**, 1–5.

79 H. N. Achmad, H. E. Rana, I. Fadilla, A. Fajar, R. Manurung and M. Y. Abduh, *J. Chem. Nat. Res. Eng.*, 2018, **1**, 36–49.

80 T. H. Tran, T. C. Q. Ngo, T. P. Dao, P. T. N. Nguyen, T. N. Pham, T. D. Nguyen, H. T. K. Linh, N. H. Nguyen and M. H. Cang, *IOP Conf. Ser.: Mater. Sci. Eng.*, 2020, **736**, 022040.

81 N. Abbasi, Z. Khalighi, Z. Eftekhari and M. Bahmani, *Adv. Anim. Vet.*, 2020, **8**, 647–652.

82 K. Yuan, F. Li, L. Peng, X. Zhao and H. Song, *J. Mol. Liq.*, 2022, **350**, 118516.

83 K. A. Santos, C. M. de Aguiar, E. A. da Silva and C. da Silva, *J. Supercrit. Fluids*, 2021, **169**, 105125.

84 D. Panda and S. Manickam, *Appl. Sci.*, 2019, **9**, 766.

85 S. Sharifzadeh, S. Karimi, H. Abbasi and M. Assari, *J. Food Meas. Charact.*, 2021, **16**, 377–390.

86 R. Richa, R. Kumar, R. M. Shukla and K. Khan, *SKUAST J. Res.*, 2020, **22**, 78–85.

87 J. Danlami, A. Arsad, M. Ahmad Zaini and H. Sulaiman, *Rev. Chem. Eng.*, 2014, **30**, 605–626.

88 A. Martínez-Abad, M. Ramos, M. Hamzaoui, S. Kohnen, A. Jiménez and M. C. Garrigós, *Foods*, 2020, **9**, 1493.

89 S. Khruengsai, N. Promhom, T. Sripahco, P. Siriwat and P. Pripdeevech, *Sci. Rep.*, 2023, **13**, 12872.